

Alternative View of Long Chain Branch Formation by Metallocene Catalysts

Qing Yang,[†] Michael D. Jensen,[‡] and Max P. McDaniel^{*,†}

[†]*Chevron-Phillips Research Department, Bartlesville, Oklahoma 74004, and*

[‡]*Grace Davison Specialty Catalysts, Columbia, Maryland 21044-4009*

Received July 1, 2010; Revised Manuscript Received August 12, 2010

ABSTRACT: The widely accepted mechanism of long chain branch (LCB) formation, i.e. random macromer incorporation, conflicts with many of the experimental trends observed in polyethylene production. This includes the response of LCB to common reactor variables, the surprisingly high LCB incorporation efficiency, and in particular the effect of metallocene structure on LCB levels. Many metallocenes are known to produce comparatively high amounts of LCB, while others produce little or none. In contrast to expectations from the widely accepted mechanism, this frequently has little to do with the site's ability to incorporate comonomer. Instead, LCB and SCB (short chain branch) incorporation are found to be relatively independent of each other. These problems are addressed and a modification of the LCB mechanism is proposed, that is *intra-* versus *intermolecular* macromer incorporation. The consequences of the proposed *intramolecular* insertion are discussed, including the effect of metallocene structure on LCB and SCB incorporation. The ability of a metallocene site to incorporate LCB may be mainly determined, not by its ability to incorporate comonomer, but rather by its ability to coordinate and hold on to terminated macromer. Consistent with *intramolecular* LCB formation, no evidence was found in slurry polymerization experiments of cross-insertion between sites, i.e., the incorporation by one site of macromer produced from another site. This has implications for the predicted architecture of polyethylene (e.g., Y's, trees, combs, etc.).

Introduction

Metallocene catalysts often tend to produce long chain branching (LCB) during the polymerization of ethylene.^{1–8} It is almost universally accepted that this happens when vinyl groups on the end of terminated chains become incorporated into another growing chain as a branch (Scheme 1). Such “macromonomer” (often shortened as “macromer”) incorporation occurs infrequently, producing perhaps only a few branches per one million total carbons, but that is enough to have profound consequences for PE molding characteristics and final properties. For example LCB governs die swell, melt strength, and environmental stress crack resistance in blow molding operations, bubble stability and lamellae orientation in film, sag resistance in pipe and geomembrane, and shear thinning and melt fracture in all extrusion processes. Consequently a major objective of commercial catalyst research is to control LCB formation.

The mechanism of LCB formation is widely regarded as a random *intermolecular* reaction. That is, vinyl end-groups react with active sites in the same way that any other comonomer would, i.e., like the 1-hexene used to produce short chain branching (SCB). Thus, the production of LCB, like SCB, should be determined by (1) the reactivity of the site toward comonomer, (2) the reactivity of the comonomer, and (3) the relative concentrations of comonomer and ethylene. This seems intuitive in a solution process, where macromer is dissolved in a solvent as it is formed (Scheme 1A). One can speak of macromer concentrations in the usual sense, because these macromers are in solution and have access to active sites. However, in a slurry or gas phase process, the polymer does not go into solution, but instead is frozen into a solid matrix as it is formed (Scheme 1B). Therefore,

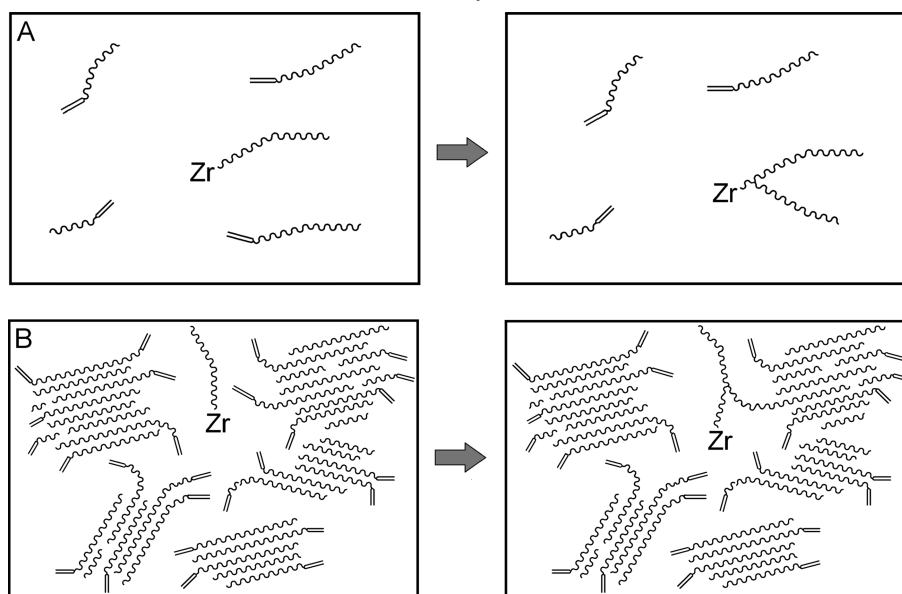
it is not clear how macromers randomly come into contact with active sites. Surprisingly, this immobilization does not prevent the macromer from incorporating to form LCB.² This problem has not been addressed in the literature. One can speculate that while most of the chain may be cocrystallized into the solid matrix, the vinyl end-groups are probably concentrated into the amorphous regions of the polymer. Consequently, one must assume that they have some limited mobility that allows access to the active sites that are also buried in the amorphous regions (Scheme 1B). This would tend to concentrate the vinyls into a small space, perhaps enhancing their reactivity.² Indeed it was reported that, for chromium and metallocene catalysts, polymers made in the solution process tend to incorporate less LCB than those made in the slurry process.^{2,9–11}

Nevertheless, many of the LCB trends observed experimentally are not in agreement with predictions from the widely accepted conventional mechanism of LCB formation as presented in Scheme 1A or Scheme 1B. Some of these contrary observations have been described in previous reports for Phillips chromium oxide catalysts, including the unanticipated effect of reactor variables on LCB^{9–11} and the effect of catalyst porosity on LCB.^{10–13} In this paper, still more of these counterintuitive responses are documented, this time for metallocene catalysts in a slurry process. A modification of the conventional mechanism is proposed that is more consistent with experimental observation. We describe the new mechanism as “*intramolecular*”, in contrast to “*intermolecular*”, incorporation of macromer, and evidence for this mechanism is presented and discussed.

Experimental Section

Catalyst Formation. Most metallocenes used in this study were obtained from Boulder Scientific. This includes the entries 1, 2, and 5 in Table 2, all entries in Table 3, and entry 1 in Table 4.

*To whom correspondence should be addressed. E-mail: Max.McDaniel@sbglobal.net.

Scheme 1. Conventional Mechanism of Macromer Incorporation to Produce Long Chain Branching in (A) Solution Polymerization and (B) Slurry or Gas Phase Polymerization**Table 1. LCB Levels in Polymers Made from Three Different Metallocene Catalysts as a Function of the 1-Hexene Concentration in the Reactor^a**

Metallocene	1-Hexene Concentration, mol/L						
	0.05	0.10	0.13	0.16	0.21	0.23	0.26
		30		2	1		1
	7	7		2	1		1
	3	3		1		0.3	

^a LCB listed as branches per million total carbons; reaction conditions of 90 °C, *i*-C₄H₁₀, and 3.8 MPa ethylene.

Table 2. Influence of Metallocene Bridge Structure on SCB and LCB Incorporation^a

Metallocene Structure					
1-Hexene Incorp. Eff.	0.097	0.086	0.052	0.037	0.035
LCB/10 ⁶ C [*]	100	22	0.5	0.3	0.2
CY-a	0.0729	0.2086	0.6248	0.6279	0.6377

^a The asterisk indicates data determined rheologically through the Janzen–Colby relationship.

C3- and C4-bridged racemic indenyl zirconium dichlorides in Table 2 were synthesized according to ref 14, while metallocenes 2 and 3 in Table 4 were synthesized according to refs 15 and 16. The activator support was a fluorided silica–alumina made according to refs 17–20.

Polymerization Runs. Most ethylene polymers used in this study were prepared in a continuous slurry process by contacting

Table 3. Influence of Metallocene Ring Substituent on SCB and LCB Incorporation^a

Metallocene Structure					
1-Hexene Incorp. Eff.	0.041	0.039	0.037	0.038	0.038
LCB/10 ⁶ C [*]	100	9.5	3.5	0.5	0
CY-a	0.0706	0.1961	0.2333	0.6543	0.7132

^a The asterisk indicates determined rheologically through the Janzen–Colby relationship.

Table 4. Influence of Metallocene Bridge Substituent on SCB and LCB Incorporation

Metallocene Structure			
1-Hexene Incorp. Eff.	0.11	0.13	0.12
LCB/10 ⁶ C			
By Rheology	100	100	1
By SEC-MALS	nd	80	3
CY-a	0.0521	0.0652	0.6543
Activity, kg/g-h	154	167	479

a catalyst with ethylene and 1-hexene. The medium and temperature are thus selected such that the copolymer is produced as solid particles and is recovered in that form. The ethylene was obtained from Dow Corporation as polymerization grade, and was further purified over activated 13X molecular sieve. Isobutane was degassed by fractionation and also dried over molecular sieves.

The reactor was a 15.2 cm diameter pipe-loop, having a volume of 87 L. Liquid isobutane was used as the diluent at a pressure of 4.14 MPa so that no gas pockets formed. Hydrogen

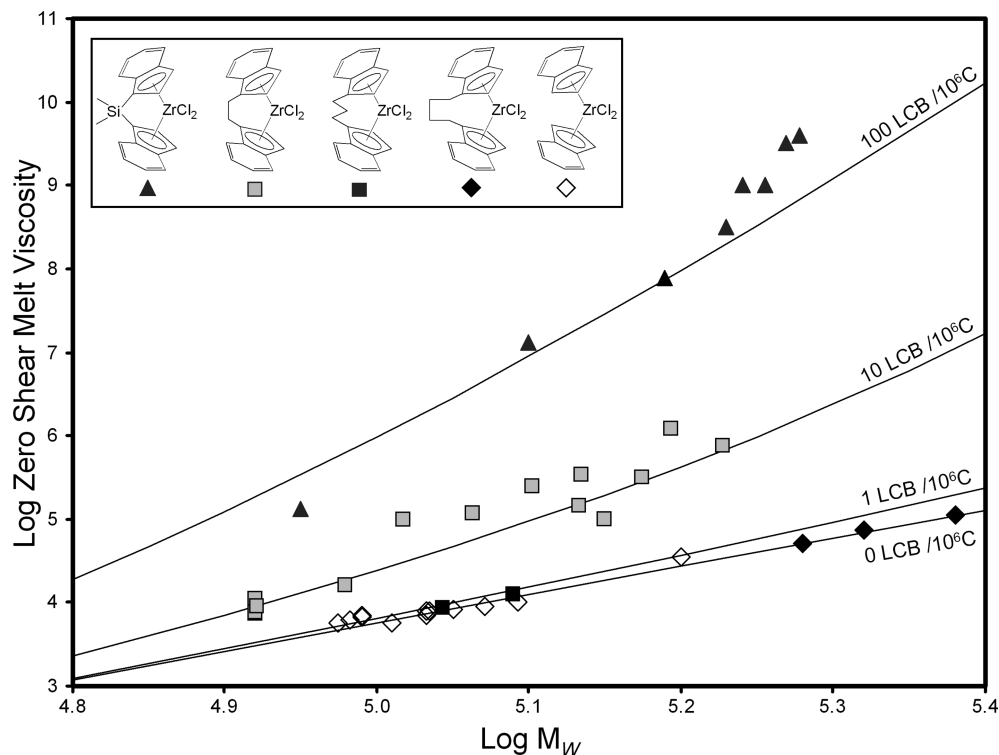


Figure 1. Janzen–Colby plot of polymers made with bridged metallocenes.

was sometimes added to regulate the molecular weight of the polymer product. The reactor temperature was set at 82 °C, and it was operated to have a residence time of 1.25 h. Activator support was added through a 0.35 cm³ circulating ball-check feeder. At steady state conditions the isobutane feed rate was about 46 L per hour, the ethylene feed rate was about 14 kg/h, and the 1-hexene feed rate was varied to control the density of the polymer product to 0.918 g/mL. Ethylene concentration in the diluent was 10–12 mol percent. Cocatalysts such as triethylaluminum (Tables 2 and 3) and triisobutylaluminum (Table 4) were added at 10–30 ppm.

A few polymerizations were carried out in a one gallon stirred Autoclave Engineers laboratory reactor. After purging, about 0.1–0.2 g of activator support was charged to the reactor under nitrogen, followed by 0.001 to 0.003 g of metallocene, and then 1 mL of 1 M trialkylaluminum cocatalyst. Next 1-hexene was injected into the reactor, followed by two liters of isobutane liquid. The reactor was subsequently heated to 80 °C, stirred at 700 rpm, and then ethylene was added to the reactor and fed on demand to maintain a fixed total pressure of 450 psig. The reactor was maintained at the specified temperature for about 30 min. Then the isobutane and ethylene were vented from the reactor, which was opened, and the polymer was collected as a dry powder.

Rheology Measurements. Samples for viscosity measurements were compression molded at 182 °C for a total of 3 min. The samples were allowed to melt at a relatively low pressure for 1 min and then subjected to a high molding pressure for an additional 2 min. The molded samples were then quenched in a cold (room temperature) press. The 2 mm × 25.4 mm diameter disks were stamped out of the molded slabs for rheological characterization. Fluff samples were stabilized with 0.1 wt % BHT dispersed in acetone and then vacuum-dried before molding.

Small-strain oscillatory shear measurements were performed on a Rheometrics Inc. rms-800 or ARES rheometer using parallel-plate geometry over an angular frequency range of 0.03–100 rad/s. The test chamber of the rheometer was blanketed in nitrogen in order to minimize polymer degradation. The rheometer was preheated to the initial temperature of the study.

Upon sample loading and after oven thermal equilibration, the specimens were squeezed between the plates to a 1.6 mm thickness and the excess was trimmed. A total of approximately 8 min elapsed between the time the sample was inserted between the plates and the time the frequency sweep was started.

Strains were generally maintained at a single value throughout a frequency sweep but larger strain values were used for low viscosity samples to maintain a measurable torque. Smaller strain values were used for high viscosity samples to avoid overloading the torque transducer and to keep within the linear viscoelastic limits of the sample. The instrument automatically reduces the strain at high frequencies if necessary to keep from overloading the torque transducer. These data were fit to the Carreau–Yasuda equation to determine zero shear viscosity (η_0), relaxation time (τ), and a measure of the breadth of the relaxation time distribution (CY- a).²¹

Molecular Weight. Molecular weights and molecular weight distributions were obtained from a Waters 150 CV Plus or a Polymer Laboratories PL220 gel permeation chromatograph using trichlorobenzene as the solvent with a flow rate of 1 mL/min at a temperature of 140 °C. BHT at a concentration of 0.5 g/L was used as a stabilizer in the solvent. An injection volume of 220 μ L was used with a nominal polymer concentration of 6.5 mg/3.5 mL (at room temperature). The column set consisted of two Waters Styragel HT 6E mixed-bed or three or four PLGel Mixed A columns plus a guard column. A broad-standard integral method of universal calibration was used based on a Phillips Marlex BHB 5003 broad linear polyethylene standard. Parameter values used in the Mark–Houwink equation ($[\eta] = KM^a$) for polyethylene were $K = 39.5(10^{-3})$ mL/g and $a = 0.726$.

Rheological Analysis of LCB Content. To be rheologically significant, a branch must be longer than the critical entanglement length, which for polyethylene is known to be about 140 carbons.^{22,23} It is very difficult to estimate LCB levels, position, or length, in commercial PE products. NMR cannot be used for this purpose. Size exclusion chromatography multiangle light scattering (SEC–MALS) can detect LCB at high levels, and can even provide an LCB distribution within the MW distribution. In several experiments SEC–MALS was used as a secondary

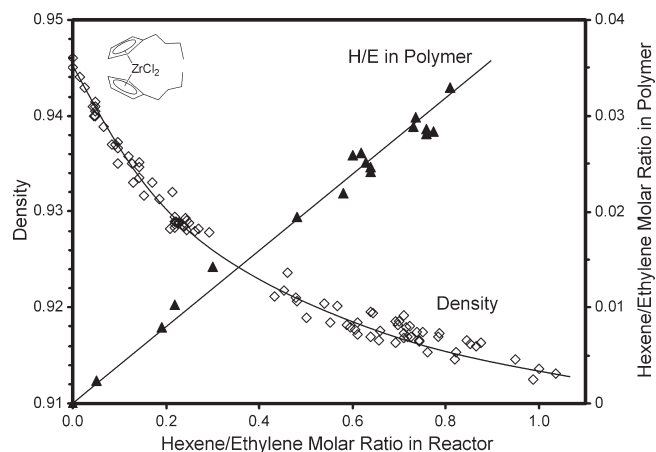


Figure 2. 1-Hexene incorporation as a function of reactant concentration.

indication of LCB, however, SEC–MALS is not very sensitive to LCB in the low-MW part of the distribution.

Melt rheology is very sensitive to the effects of LCB, even at trace levels.^{24,25} Chains containing LCB entangle in the melt phase, profoundly increasing the low shear melt viscosity. Therefore, the most sensitive method of gauging LCB is to look for increases in low shear melt viscosity that go beyond what would be expected from linear polymers of the same molecular weight. Like many other polymers, PE having no LCB follows a log dependence of melt viscosity on molecular weight. If the log of the extrapolated zero-shear viscosity (designated η_0) is plotted against the log of the weight-average molecular weight (M_w), a straight line is obtained having a slope of 3.4. The presence of LCB is indicated by deviations from this “power law” or Arnett line.^{9,22,21,26,27} Many Arnett plots are presented below (see, for example, Figure 2). The Arnett line running diagonally near the bottom and labeled “0 LCB/C”, indicates the position of polyethylene having no long chain branches. Deviations above the line indicate that traces of LCB are present.

The effect of LCB on viscosity is more pronounced at high MW than at low MW, because entanglements are less easily overcome during flow. This relationship was defined by Janzen and Colby, giving rise to the curved contour lines for given LCB levels on these plots (see again, for example, Figure 2).²² This insight provides a helpful reference to compare LCB levels in polymers at different molecular weights. At very low MW, e.g., M_w of 10 000, the effects of LCB become much less pronounced.

Unfortunately this method also comes with some caveats, most notably the effect of MW breadth. Thus, a small correction according to Yau²⁷ was applied in some cases where the polydispersity was higher than the usual 2.0.

SEC–MALS Analysis of LCB Content. LCB content was also obtained through a combined method of size exclusion chromatography (SEC) with multiangle light scattering (MALS). In the SEC–MALS system used in this study,²⁸ a DAWN EOS photometer (Wyatt Technology, Santa Barbara, CA) was attached to a Waters 150-CV plus GPC system (Waters, Milford, MA) or a PL-210 GPC system (Polymer Laboratories, now part of Varian) through a hot-transfer line controlled at 145 °C. Degassed mobile phase, 1,2,4-trichlorobenzene that contains 0.5 wt % of BHT (TCB) was pumped through an inline filter before passing through the SEC column bank. Polymer solutions injected to the system were brought downstream to the columns by the mobile phase for fractionation. The fractionated polymers first elute through the MALS photometer where light scattering signals are recorded before passing through the differential refractive index detector (DRI) where their concentrations are quantified.

The DAWN EOS system was calibrated with neat toluene at room temperature to convert the measured voltage to intensity

of scattered light. During the calibration, toluene was filtered with 0.02 μm filter (Whatman) and directly passed through the flowcell of the MALS. At room temperature, the Rayleigh ratio at the given conditions was given by $1.406 \times 10^{-5} \text{ cm}^{-1}$.²⁹ A narrow polystyrene (PS) standard (American Polymer Standards) of MW of 30 000 g/mol and a concentration of 5–10 mg/mL in TCB was employed to normalize the system at 145 °C. At the given chromatographic conditions, radius of gyration (R_g) of the polystyrene (PS) was estimated to be 5.6 nm using Fox–Flory equation coupled with its Mark–Houwink exponent in the chromatographic conditions.^{30,31}

At a flow rate set at 0.7 mL/min (actual flow rate: 0.60–0.65 mL/min), the mobile phase was eluted through three 7.5 mm \times 300 mm 20- μm mixed A columns (Polymer Laboratories). PE solutions with nominal concentrations of 1.0–1.2 mg/mL were prepared at 150 °C for 3–4 h before being transferred to GPC injection vials sitting in the carousel heated at 145 °C. In addition to a concentration chromatogram, 17 light scattering chromatograms at different angles were also acquired for each injection. At each chromatographic slice, both the absolute molecular weight (MW) and the root-mean-square radius, also known as radius of gyration, R_g , were obtained from Debye plots.³² The linear PE reference employed in this study was HiD9640, a high density PE with broad MWD (Chevron Phillips Chemical). Refractive index increment dn/dc used in this study was 0.097 mL/g for PE dissolved in TCB at 135 °C.³³

Results and Discussion

LCB Vs. Common Reactor Variables. In the conventional (intermolecular) mechanism, LCB formation is considered as a copolymerization in which macromer is just a very large comonomer. Therefore, the usual rules of copolymerization should apply. For example, LCB incorporation, like SCB incorporation, should vary inversely with reactor ethylene concentration. Indeed, this trend has been observed in experimental data, from this laboratory and others. That is, LCB levels do usually increase with decreasing ethylene concentration.^{4,34–36} Thus, in this case, the conventional mechanism does seem to be consistent with observation.

However, the LCB response to other reactor variables contradicts what would be predicted from the conventional (intermolecular) mechanism. For example, increasing the reactor temperature should lower the MW, thus increasing the vinyl end-group concentration. Higher temperature should also make those vinyl groups more mobile within the amorphous regions of the polymer. Together, according to Scheme 1A or Scheme 1B, these trends would be expected to increase LCB levels. However, we have not observed an increase in LCB level with reactor temperature for any metallocene tested.

For example, Figure 1 shows a typical Janzen–Colby plot from various metallocenes. It is a log–log plot of zero-shear melt viscosity against molecular weight. Linear polymers fall on the linear reference line, while small amounts of LCB cause a positive deviation.^{9,22,26} The greater the deviation, the more LCB, but that deviation is also a function of MW so it must be interpreted in relation to the Janzen–Colby gridlines shown in the graph. Each Janzen–Colby grid line represents a certain level of LCB.²² For each metallocene tested, the reactor temperature was also varied to produce a family of polymers of varying MW. Notice that each family of resulting points forms a line that tends to follow the Janzen–Colby gridlines. This indicates a constant LCB frequency within each family, independent of MW, and contrary to the conventional mechanism in Scheme 1A or Scheme 1B. Others have reported that raising reactor temperature *decreases* LCB.^{2,36} The Figure 1 results are also consistent with Phillips Cr/silica

catalysts, which also produce essentially constant LCB as temperature is varied.⁹

Another common reactor variable is the 1-hexene concentration. The incorporation of 1-hexene can lead to the introduction of small amounts of vinylidene end-groups, caused by termination after insertion. In some cases 1-hexene can also enhance chain termination by acting as a better β -H receptor,¹¹ thus increasing the production of terminal vinyls. Therefore, from the conventional mechanism of LCB formation, one might expect LCB levels to be unaffected or even increased by the presence of 1-hexene. In practice, however, it is often found that adding 1-hexene to the reactor can lower LCB levels in the polymer, sometimes quite significantly. An example of this is shown in Table 1, where three different metallocenes were tested under constant conditions, except that the 1-hexene level in the reactor was varied. In the table is listed the LCB level as determined from the same Janzen–Colby method that was illustrated above in Figure 1. The log–log plot itself is included in the Supporting Information as Figure S1, and also the van Gurp–Palmen plot of delta vs complex modulus in Figure S2. Notice in Table 1 that LCB levels decline as more 1-hexene is added to the reactor. Others have also noted this same response.^{4,7,34,36–38} Therefore, once again the conventional (*intermolecular*) mechanism fails to predict experimental results.

Incorporation Efficiency. α -Olefins incorporate into PE more reluctantly than ethylene. However, some catalysts copolymerize comonomer more easily than others. In this study 1-hexene was often added to the loop reactor to maintain a given concentration in the diluent, which was continuously monitored by gas chromatography. Both 1-hexene and ethylene concentration were varied independently. Figure 2 demonstrates how the polymer density responded to reactant concentrations for one particular metallocene, bis(*n*-butylcyclopentadienyl)zirconium dichloride. The *X*-axis is the ratio of the molar concentration of 1-hexene to ethylene in the reactor. Density drops with rising reactant ratio, giving the familiar curve. A second line is also shown in the figure, representing the 1-hexene to ethylene molar ratio found by NMR in the polymer. This line passes through the origin, indicating that the amount of 1-hexene incorporated is proportional to the reactant ratio. Therefore, the incorporation selectivity is first order. The term “incorporation efficiency” is used throughout this paper to compare one catalyst to another, or one comonomer to another. We define it as the slope of this line. For comparing metallocenes, this is the value that is listed in Tables 2–4. For consistency this was usually obtained by driving the density down to about 0.918 g/mL.

SCB/LCB Incorporation vs Metallocene Structure. Another problem with Scheme 1B is the SCB/LCB response of one metallocene relative to another. If macromer is regarded like other comonomers in a conventional (*intermolecular*) copolymerization, then one expects parallel reactivity from active sites toward SCB and LCB. That is, sites that easily incorporate 1-hexene would also tend to produce higher levels of LCB and vice versa. This relationship has been almost universally accepted in the literature.^{34,36,39} Modifications to the metallocene structure that affect SCB incorporation, such as changing the gap aperture, are expected to similarly influence LCB incorporation.

Early explorations of metallocene catalysts seemed to confirm this expectation. One structural feature that has a profound effect on SCB incorporation is the bridge linking the two rings together.^{4,40} Tightly bridging the two rings greatly improves the efficiency of 1-hexene incorporation. This is usually explained in steric terms. That is, tight

bridging pulls the rings back, thus increasing the gap aperture, making the zirconium cation more accessible to encumbered comonomers.⁴⁰ Electronically, pulling the rings back may also create more positive charge on the zirconium due to decreased ligand-to-metal π -electron donation. This in turn may also yield a stronger relative affinity toward α -olefin than ethylene, the α -olefin being a better π -electron donor than ethylene. With either explanation, there is nothing that would allow the site to preferentially discriminate for or against macromer versus 1-hexene. Therefore, according to the purely random (*intermolecular*) Scheme 1A or Scheme 1B, one should expect that metallocene structural changes would affect SCB and LCB incorporation similarly.

An example of this behavior is shown in Table 2. In this series, racemic indenyl complexes are bridged, at first tightly by a single silicon atom, then ever more loosely as the bridge expands to two, three, and then four carbons. The final member of the series has no bridge at all. Under each structure in Table 2 is the 1-hexene incorporation efficiency, as illustrated by the slope in Figure 2 above. Notice that the 1-hexene incorporation decreases by a factor of 3 over the series as the bridge is relaxed, and the effective gap aperture decreased. Considerable relative lateral rotation of the rings is permitted in progressing from the 1- to 4-atom bridge.^{40–45} Of course, the final unbridged member allows independent free rotation of the rings.

Listed in Table 2 is the LCB level produced by these metallocenes. As noted above, this was measured using the Janzen–Colby method, illustrated in Figure 1. Again, it is a log–log plot of zero-shear melt viscosity against molecular weight. Linear polymers fall on the linear reference line, while small amounts of LCB cause a positive deviation.^{9,22,26} The degree of LCB can be gauged from the amount of deviation, relative to the Janzen–Colby grid lines.²² An average value from many points is listed in Table 2 under each structure. Also listed in Table 2 is the Carreau–Yasuda “*a*” parameter, which is a measure of the relaxation time distribution of the polymer. LCB tends to contribute molecules that relax more slowly, thus broadening the distribution of relaxation times. If the MW and MW distribution are similar, as in these examples, then the CY-*a* value may be taken as another indication of LCB. Decreasing CY-*a* indicates greater LCB.

Notice in Table 2 and Figure 1 that when the gap aperture is large, macromer incorporation, like 1-hexene incorporation, increases. The elasticity of the polymer gradually decreases (LCB level goes down) as the bridge length increases giving a smaller effective gap aperture. The freely rotating indenyl rings of the unbridged metallocene, and the complex with the longest bridge, thus yield the lowest LCB levels. Similarly, the CY-*a* value increases. Consequently, in this series the expectation from the conventional (*intermolecular*) mechanism of LCB formation in Scheme 1A and 1B seems to be justified, at least qualitatively. That is, LCB and SCB incorporation do trend similarly with respect to systematic changes in the metallocene. Structural factors influencing SCB formation have a similar effect on LCB formation. However, on a quantitative level, the relationship is less satisfying. Notice that while SCB efficiency drops by a factor of 3, LCB formation drops by almost 3 orders of magnitude.

Thus, the expected parallel behavior between SCB and LCB incorporation is not always observed. In fact it is contradicted by many other observations. One example is shown in Table 3. In this series, all the metallocenes contain two unbridged cyclopentadienyl rings. A single substituent on the rings is varied from H to methyl, then ethyl, *n*-propyl, and finally *n*-butyl. Again the 1-hexene incorporation efficiency is listed

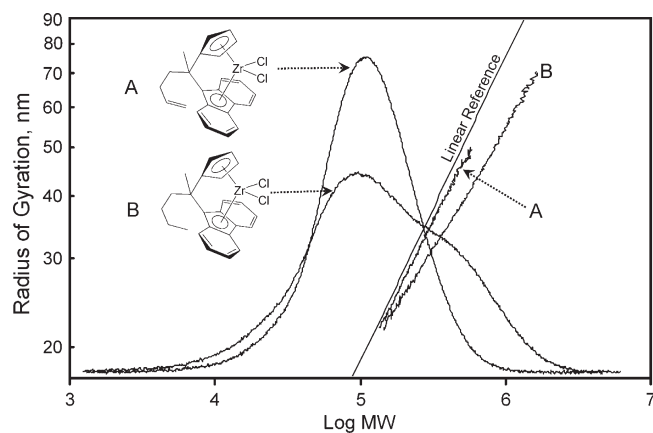


Figure 3. SEC-MALS results for two polymers obtained with two metallocenes differing only in one substituent on the bridge.

below each metallocene, and one response was also plotted in Figure 2 above. In this series there is very little difference in 1-hexene incorporation between the members. Typical of unbridged metallocenes, all exhibited relatively poor incorporation of 1-hexene, compared to the tightly bridged metallocene in Table 2. However, the LCB formation, which is also shown in the table below each member, varies widely over the series, as does the CY-a value. As the substituent alkyl becomes larger, LCB levels drop, reaching near zero for $(n\text{-BuCp})_2\text{ZrCl}_2$. Others have reported similar trends.^{46–48} Apparently substituent bulk hinders LCB formation, without affecting SCB incorporation. In this series it is clear that SCB and LCB incorporation behave independently with respect to systematic perturbations of metallocene structure. LCB formation can be varied widely without any effect on SCB formation, perhaps suggesting different mechanistic pathways for macromer versus 1-hexene incorporation.

Another example that contradicts an identical mechanistic pathway for SCB and LCB incorporation is shown in Table 4. In contrast to the series in Table 3, each metallocene possesses a cyclopentadienyl ring tightly bridged by a single carbon to a fluorenyl ring, thus exhibiting a large gap aperture. A single substituent on the bridge was varied within the series, from methyl to *n*-butyl to *n*-butenyl. Again the 1-hexene incorporation efficiency is listed below each metallocene. As expected, and consistent with the tightly bridged example in Table 2, all of the members in this series exhibit excellent 1-hexene incorporation efficiency. All were about 3–4 times more efficient than the unbridged metallocenes in Table 3. Unexpectedly, however, the LCB level, as indicated by the Janzen–Colby treatment of rheological measurements, and also by CY-a values, varied widely over the series, dramatically decreasing when the bridge substituent contained a pendant vinyl group.⁴⁹

SEC-MALS analysis of the polymer indicated a similar conclusion. The radius of gyration for two of the polymers in Table 4 is plotted against molecular weight in Figure 3. Polymers that are highly branched exhibit a smaller radius of gyration in solution than linear polymers for a given MW. Note that the pendant olefin on the metallocene structure results in a larger radius of gyration in the polymer, indicating that long chain branching has been significantly reduced. A linear reference is also shown for comparison. All three lines merge at the lower-MW side of the MW distribution due to the inherent limitations of the SEC-MALS technique. Using the Zimm–Stockmayer approach,⁵⁰ these SEC-MALS measurements were then translated into the actual LCB content, which is listed in Table 4 at the weight-average MW. These

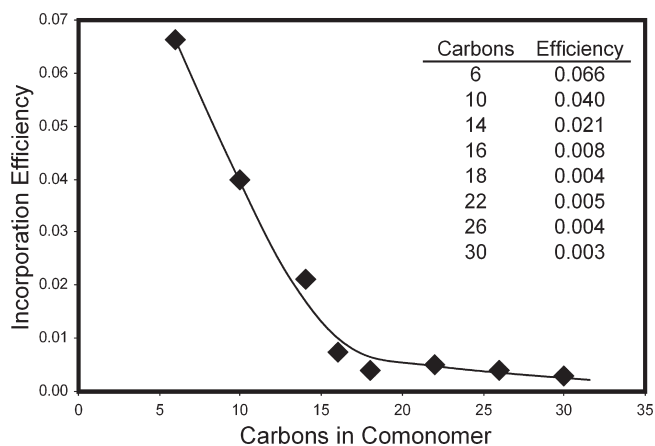


Figure 4. Influence of comonomer type on incorporation efficiency.

values are very close to those obtained from the rheology, again indicating that the pendant olefin tends to strongly inhibit LCB formation. No great differences were observed in the vinyl end-group concentration in both polymers. Thus, Table 4 shows another series in which SCB and LCB formation appear to follow different mechanistic pathways not readily predicted by the conventional view of random, *intermolecular* comonomer/macromer incorporation.

The examples described above are only a few of the dozens of metallocene series from our work and others that could be cited to demonstrate the independent behavior of LCB versus SCB incorporation. Many other metallocenes containing tethered olefins have also been prepared and tested in this laboratory, showing similar performance to Table 4.^{16,49,51} That is, the complexes containing tethered olefin substituent tend to shut down LCB without affecting SCB. Similarly, substituents of sufficient length extending from the front of the ring of tightly bridged metallocenes (i.e., anti to the bridge) have also been found to retard LCB with little effect on SCB.^{46,52,53} Thus, contrary to the conventional mechanism of Scheme 1A or Scheme 1B, some metallocenes incorporate comonomer very efficiently but do not produce LCB, while others incorporate comonomer poorly but produce high levels of LCB.

Incorporation Efficiency of Large Comonomers Vs. LCB.

The relative incorporation efficiency of LCB for these metallocenes can also be compared to that of higher α -olefins. Various α -olefins were tested with two of the unbridged metallocenes in Table 3, specifically Cp_2ZrCl_2 and $(n\text{-BuCp})_2\text{ZrCl}_2$. The test was done like that in Figure 2, except at 90 °C rather than 80 °C, which tends to increase the α -olefin incorporation efficiency somewhat. The results are summarized in Figure 4 for the latter metallocene. The former provided a very similar plot. The incorporation efficiency was computed as in Figure 2, from the slope of the line, i.e., the comonomer to ethylene ratio in the polymer divided by that in the reactor. One can see that longer α -olefins tend to be less reactive, as would be expected from entropic considerations.⁵⁴ The slope of this downward line can be affected by metallocene type and reactor conditions, but it will nevertheless always extrapolate to some low value, which in this case occurred between C18 and C30 comonomers. The relative reactivity of different metallocenes with 1-hexene is paralleled with higher α -olefins as well.⁴

The largest α -olefin tested in this series was a C30 alkene, which exhibited only about 3% of the reactivity of 1-hexene. Therefore, one might expect LCB incorporation, which involves olefins longer than 150 carbons and mostly immobilized by crystallization in a solid matrix, to be much more

difficult to incorporate. Assuming the convention (*intermolecular*) mechanism of LCB formation, one can make an estimate of the incorporation efficiency of LCB. For example, the LCB level produced by the metallocenes in Table 3 reached up to 100 branches/ 10^6 carbons for the first member of the series, Cp_2ZrCl_2 , which was also tested with large comonomers. Let us consider this case in more detail to estimate the reactant concentrations.

This amounts to an incorporation of about 200 branches per million ethylene insertions. To consider incorporation efficiency, the macromer concentration can be estimated. A typical density of 0.92 g/mL means that the polymer is about 57% amorphous (computed from reported densities of pure crystalline (1.00 g/mL) and amorphous (0.86 g/mL) components) and a typical melt index of about 1.0 corresponds to a number-average MW of approximately 40 000 g/mol. If every chain contains a vinyl end-group, this gives a vinyl end-group concentration of about 0.04 mol/L within the amorphous regions of the polymer. [Actual vinyl end-group concentrations are often less than one per chain, due to the formation of H_2 during polymerization. Using a smaller number increases the calculated incorporation efficiency still further.] The macromer/ethylene ratio incorporated can be divided by the term-vinyl/ethylene reactant ratio to obtain an incorporation efficiency of 0.0101. This is listed in Table 5, along with other, similar calculations for other polymers, all having 100 LCB/ 10^6 carbons. Thus, Table 5 lists the incorporation efficiency needed to produce 100 LCB/ 10^6 carbons, at different densities and molecular weights. Higher MW means lower vinyl mol/L reactant concentrations, thus requiring higher efficiency to yield the same LCB level. Lower density means that the polymer takes up more space, and has a larger proportion of amorphous polymer. term-vinyl mol/L concentration is thus diluted and higher incorporation efficiency is needed to maintain a constant LCB level.

Table 5. LCB Incorporation Efficiencies^a Calculated for 100 LCB/ 10^6 Carbons at Various Densities and Molecular Weights

$M_N/1000$	density			
	0.95	0.94	0.93	0.92
40	0.0061	0.0074	0.0087	0.0101
80	0.0122	0.0148	0.0175	0.0202
120	0.0183	0.0222	0.0262	0.0303
150	0.0229	0.0278	0.0327	0.0378

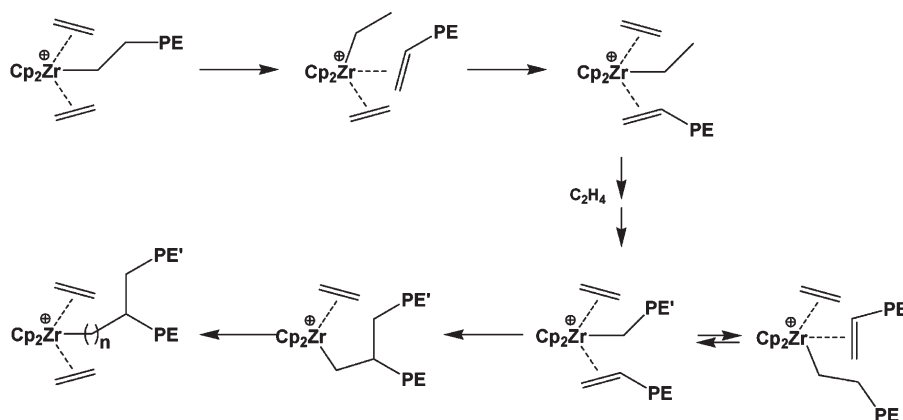
^a LCB/ethylene ratio in polymer divided by term-vinyl/ethylene reactant ratio near active site. Reactant concentrations based on 1 term-vinyl per chain contained in the amorphous regions of the polymer, and ethylene concentration equal to that in the isobutane diluent.

It is interesting to compare the typical LCB incorporation efficiencies in Table 5 to that of the longest α -olefin comonomer tested in Figure 4. All the values in Table 5 are larger than the C30 efficiency in Figure 4. This means that, in this case, LCB incorporates more easily than C30. In fact, an immobilized macromer of (for example) 1000 carbons is up to 13 times more reactive than C30 α -olefin in free solution! Alternatively, the LCB incorporation efficiency is up to half that of 1-hexene. This relatively high efficiency for macromer incorporation is most unexpected. Others have also noticed this phenomenon.⁵⁵ It indicates that macromer incorporation, unlike SCB, probably occurs through some other mechanistic pathway that leads to enhanced macromer reactivity.

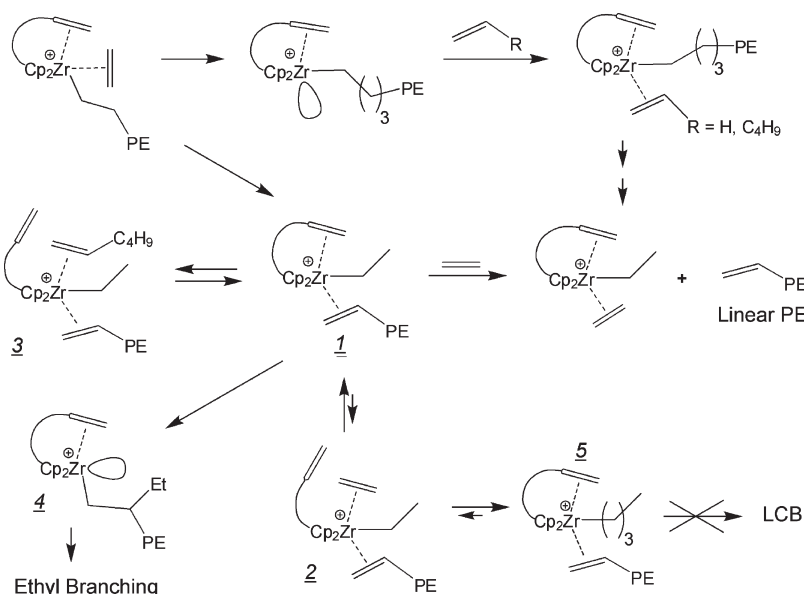
Intra- vs Intermolecular Incorporation. As demonstrated in the aforementioned examples, SCB and LCB can respond independently to systematic changes in the metallocene structure. And the widely accepted mechanism in Scheme 1A or Scheme 1B does not adequately predict experimental behavior. This includes not only the independent response of LCB and SCB to structure, but also the effect of reactor variables on LCB formation, and the surprisingly high macromer incorporation efficiency compared to comonomer. Taken together, these observations indicate that SCB and LCB incorporation can proceed through different pathways, and metallocene structure can independently influence both SCB and LCB incorporation efficiency. Comparing Tables 2–4, some high-LCB producing metallocenes incorporate SCB less efficiently than other low-LCB-producing metallocenes, and vice versa. Thus, the widely accepted (*intermolecular*) mechanism of LCB formation in both parts of Scheme 1 appears inadequate for predicting many experimental results.

By contrast, invoking a modified, *intramolecular* macromer insertion mechanism resolves the apparent problems posed by the conventional mechanism. This *intramolecular* macromer insertion mechanism is illustrated in Scheme 2. As depicted, the macromer may remain coordinated to a site during subsequent chain growth, which would imply that the metallocene cation can coordinate three ligands, in addition to the two rings,^{56,57} and that it has a propensity to coordinate two olefinic ligands in addition to the growing alkyl group. [Termination mechanisms that commonly require agostic H interaction also invoke an additional coordination site, that is, three ligands in addition to the two rings.]^{58,59} Scheme 2 can be thought of as a variant of the trigger mechanism^{60,61} in which two monomers simultaneously coordinate to the site, one to stabilize and activate the site, and the second to “trigger” an insertion. However, Scheme 2 is different in one regard: While Ystenes considered the coordination of the second olefin as a

Scheme 2. Proposed *intra*Molecular Mechanism for LCB Formation



Scheme 3. Possible Mechanism of LCB Inhibition by Tethered Olefin Substituent



transition state, triggering insertion of the first, Scheme 2 assumes that the activating olefin can remain coordinated to the site, even while growth continues.

This simple modification to the conventional mechanism reconciles many of the previously anomalous responses. Under Scheme 2, the tendency of a site to produce LCB is mainly determined by its ability to hold on to coordinated macromer (derived from that last terminated chain) during growth of a second chain. Of course, exchange between the two chains, via β -H termination to one another, may also be possible. Because of the affinity of the metallocene cation for the last terminated chain, Scheme 2 explains the surprisingly high macromer incorporation efficiency relative to other α -olefins in Figure 4. It also may explain why comonomer lowers LCB, since comonomer, being a better electron donor and more sterically congested than ethylene, should be more competitive at facilitating dissociation of coordinated macromer vs growth of a second chain. The exact mechanism remains unknown, but unlike comonomer in solution, once the "solidified" macromer dissociates from the site, it may be difficult or impossible for it to then re-coordinate. Note that steric bulk on the rings of unbridged metallocenes in Table 3, or toward the front of bridged metallocenes,^{46,52} also retards LCB, perhaps because they too can interfere with macromer retention during growth of a second chain. Likewise, lengthening the bridge of the racemic bis-indenyl series in Table 2, thus permitting greater lateral torsion of the rings and potential steric compression in the region of the three remaining coordination sites, achieves the same effect. Regarding reactor temperature and Scheme 2, raising the temperature would not be expected to increase LCB, and might even decrease it since macromer coordination would be weakened.

Finally, in perhaps the most dramatic fashion, and certainly of great commercial importance in terms of reactor operability, comonomer utilization, and resin properties,^{16,49,51,62,63} one can see how pendant olefins such as that shown in Table 4 could mitigate LCB formation. In Scheme 3, pendant olefin chelation serves to competitively inhibit chain growth while macromer is coordinated. The site may coordinate macromer, but since macromer dissociation is essentially irreversible, any coordinated macromer is derived from the previously terminated chain on the site, leaving a short alkyl group, e.g. ethyl in the case of termination to monomer, *viz.* **1**, or a hydride in the case of

termination to metal. Polymerization can resume by carbometallation of the macromer via **4**, resulting in the usual ethyl branching, observed even for homopolymerizations.^{64–68} For growth of a second chain to occur on the site, monomer needs to coordinate and insert into the Zr–ethyl or Zr–H bond. However, this is prevented by pendant chelation in **1**. Such chelation is likely reversible, and the equilibrium would be expected to depend on length and orientation of the pendant. Nevertheless, dissociation of the pendant is necessary for growth of a second chain. As shown in Scheme 3, pendant dissociation and co-ordination by monomer may occur to afford **2**. However, following insertion, pendant olefin is present in essentially infinite concentration relative to monomer in solution and ready to re-chelate to give **5**, and thus retard chain growth, and hence LCB formation. 1-Hexene may also coordinate the zirconocene cation when pendant olefin is temporarily dissociated to afford **3**. It may be even more effective than ethylene. But following its insertion, pendant olefin is again ready to re-coordinate and mitigate further chain growth. Moreover, coordination of 1-hexene, or perhaps even insertion of 1-hexene, is likely to promote steric congestion, and therefore dissociation of proximal macromer. Notably, when the pendant is saturated, such as for the second metallocene in Table 4, growth of a second chain would not be prevented, and indeed, LCB formation is facile.

In summary, as shown in Schemes 2 and 3, LCB formation may require that chain growth occurs while the metallocene cation is coordinated to the most recently terminated chain of the site. Aside from the newly initiated chain and bound macromer, this requires an additional coordination site for incoming monomer. Steric factors which favor dissociation of macromer during growth of a second chain will reduce LCB formation, as will a nonpolymerizable, constrained pendant olefin with the potential to block growth of the new chain.

Kinetics of Polymerization. The kinetics of polymerization provides other evidence that the zirconium site can be pentacoordinate, at least in a transition state, and therefore potentially able to hold on to a terminated chain. Although 1-hexene incorporates poorly into the growing chain compared to ethylene, it nevertheless has a powerful influence on ethylene incorporation.^{69–73} Figure 5 shows how the polymerization rate, which is ~98% ethylene, accelerates when a small amount of 1-hexene is added to the reactor. Three of

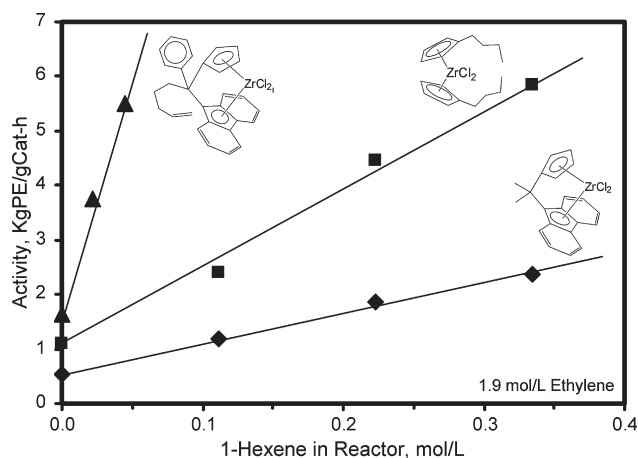


Figure 5. Enhancement of ethylene polymerization by metallocene when 1-hexene comonomer is added to the reactor.

the metallocenes used above are shown in Figure 5 as examples. Others behaved similarly. In these experiments 1-hexene was added to the reactor while the ethylene concentration was held constant. 1-Hexene in the reactor improved overall activity by up to 5–10 fold, even though only 2% of the polymer was 1-hexene. Note that this happened even though incorporation selectivity remained first order as shown in Figure 2. This indicates that the rate of incorporation of both monomers was similarly affected.

This behavior is typical of most metallocenes and many (but not all) Ziegler catalysts, whereas the effect is usually weak or absent on Phillips Cr/silica catalysts. It is not a result of 1-hexene insertion, whose influence at 2 mol % incorporation would be short-lived and therefore of no significance. It has sometimes been attributed to mass transport effects; i.e., the copolymer is more permeable to ethylene. However, this explanation is also not satisfying, given the magnitude of the effect, and the fact that not all catalysts respond, even though they still incorporate 1-hexene. We have also considered the possibility that comonomer awakens so-called “sleeping sites”. For example, chain transfer to metal leaves Zr–H bonds, and hydrosilyrconation of α -olefins is known to be faster than of ethylene. However, this hypothesis is inconsistent with the fact that hydrogen, which creates high levels of Zr–H sites, does not give the expected extreme loss in activity. In fact, some metallocenes that exhibit a large comonomer effect, barely display any loss in activity when hydrogen is added to the reactor. Hydrogen even enhances the activity of some metallocenes. Calculations from these considerations can be found in the Supporting Information.

Instead, one interpretation of this behavior is that 1-hexene can interact with and influence (or activate) sites even without being incorporated.^{72,74–77} In fact, the effect is not necessarily related to incorporation of 1-hexene at all, since both efficient and inefficient catalysts can exhibit a similar response. One possible explanation is that α -olefins coordinate to the site, stabilizing it, and perhaps even solvate and separate the metallocene ion-pair. As noted above, adding 1-hexene also tends to lower LCB. Tethered olefinic substituents like that on the third metallocene in Table 4 have a similar effect, enhancing the activity by up to 3-fold and retarding LCB. Adding 1-hexene during catalyst formation is not sufficient to retard LCB formation. It must also be present in the reactor during polymerization.

Since 1-hexene can accelerate activity independently of its own polymerization, one might suppose that ethylene would be capable of doing the same. Indeed, this would explain why

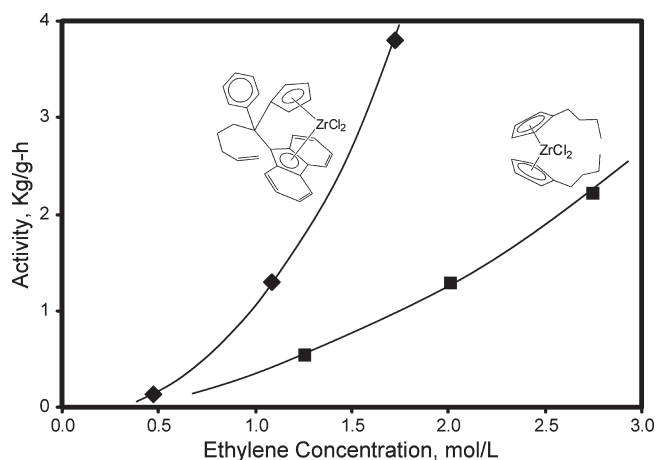


Figure 6. Activity dependence on ethylene concentration.

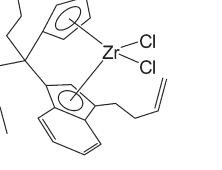
the polymerization seems to be approximately second order with respect to ethylene in these and other studies, in agreement with other reports of higher order.^{60,61,71,74,78–82} Figure 6 shows an example of this dependence for two of the metallocenes used above. Comparing Figures 5 and 6 suggests that, for a given concentration, 1-hexene has the stronger effect on activity. That is, this activity enhancement seems to be caused by relatively smaller concentrations of 1-hexene than ethylene. This may reflect the greater electron donating power of α -olefins compared to ethylene, or the greater steric bulk. Either way, it suggests that 1-hexene somehow activates the site, and that the site can simultaneously coordinate more than one olefin during polymerization.

Note that the polymerization rate in Figure 6 is approximately second order even though the incorporation selectivity remained first order as in Figure 2. As shown in Figure 2, the incorporation of 1-hexene relative to ethylene varies linearly with the reactant ratio. This does not mean that the polymerization of 1-hexene is first order with respect to 1-hexene. Actually, it is much higher order because the overall activity also increases in Figure 5. However, the straight line in Figure 2 indicates that both 1-hexene and ethylene incorporation are affected similarly by either monomer. This is a strong indication that 1-hexene (or ethylene) can activate sites, which continue to display first order dependence on monomer and comonomer.^{71,74} This reasoning also applies to ethylene. The seemingly higher order observed (one might say *pseudo* second order) is also due to the “activation” of sites, while the intrinsic dependence remains first order. This “activation” is consistent with coordination to the Zr, even as polymerization continues. Activation of sites may be due to stabilization of the electron-deficient Zr or increased ion-pair separation.

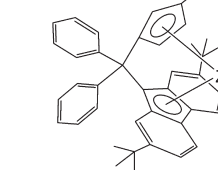
Cross-Incorporation Between Sites. Another mechanistic consideration is the behavior of catalysts containing multiple types of active sites. In the conventional *intermolecular* mechanism active sites incorporate vinyl end-groups randomly from an amorphous soup where vinyls from all sites are collectively deposited. We call this “cross-insertion” between sites, meaning that one site can incorporate chains from another site. If the catalyst system contains more than one type of active site, this has major consequences for LCB architecture. For example, active sites producing short chains can contribute up to 3 orders of magnitude more vinyls per liter than those producing long chains, even at the same polymerization rate. Therefore, if cross-incorporation can occur, broad MW distributions should provide greater opportunity for LCB formation, due to the higher vinyl mol/L concentration. The branches are likely to be relatively

Table 6. Properties of Polymers Made with Two Metallocene-Derived Components

Low MW Catalyst



High MW Catalyst



preparation method	% components			term-vinyl			JC- α LCB/10 ⁶ C
	high MW	low MW	mol wt $M_w/1000$	per 1000C ^d	per chain ^d	mol/L ^e	

a	100	0	625	0.01	0.51	0.0061	0.3
a	0	100	31	1.29	1.08	0.1107	1.2
b	55	45	378	0.58	0.85	0.0493	0.7
b	65	35	416	0.45	0.57	0.0340	0.5
b	75	25	473	0.32	0.35	0.0332	0.4
c	67	33	218	0.31	0.63	0.0535	1.5
c	67	33	230	0.29	0.67	0.0427	0.4
c	67	33	233	0.32	0.70	0.0460	0.5

^a Single polymer components made separately, each from a single metallocene catalyst. ^b Two polymer components made separately using two single component catalysts as in footnote ^a and then blended by melt extrusion. ^c Simultaneous production of two polymers through polymerization by a catalyst containing two metallocene components. ^d Based on NMR spectroscopy. ^e Based on GPC M_N , 1 vinyl per chain, and 62% amorphous

short, in comparison to backbone chains, due to the statistically disproportional vinyl content of this low-MW part of distribution. Thus, long chains should contain mostly shorter branches, affording so-called “comb” structures.

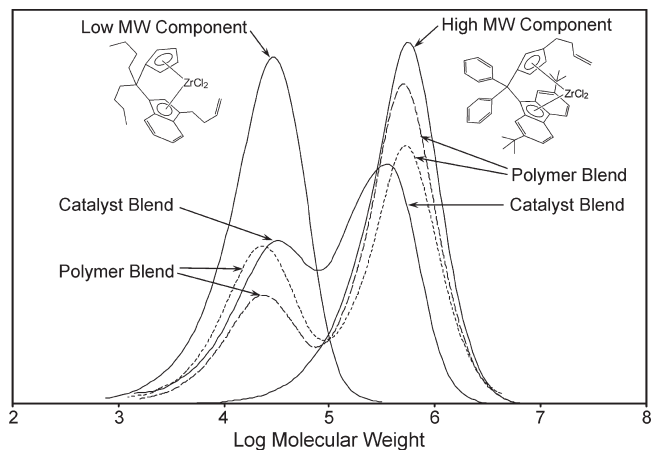
On the other hand, the *intramolecular* mechanism dictates that each site incorporates macromers produced on the same site. Therefore, long chains should incorporate mainly long branches and short chains should incorporate mainly short branches. That is, the architecture should be mostly “Y-shaped”.

The subject of cross-insertion between sites has been extensively explored in the literature. Most of these reports were attempts to mathematically model cross-insertion, and assumed a conventional, *intermolecular*, random macromer incorporation, LCB mechanism.^{39,83–92} Indeed, some have found evidence for cross insertion when the macromers are in solution.^{93–95} To our knowledge, however, there is no credible report of cross-insertion in heterogeneous polymerizations. Therefore, we searched for evidence of cross-insertion in slurry polymerizations.

To explore this issue, two metallocenes were tested, both tightly bridged and exhibiting excellent 1-hexene incorporation efficiency. Polymers were prepared in three ways. In method A, each metallocene was, in the usual way, supported alone on an activator and allowed to produce its own characteristic type of polymer. One generated low-MW polymer and the other high-MW polymer. The results of polymer testing are shown in Table 6 and the MW distributions are shown in Figure 7.

In method B these two polymers made by method A were then codissolved in various ratios in trichlorobenzene to make a bimodal polymer solution. The solution was then quickly “quenched” by adding it to an excess of cold isopropanol, thus precipitating the bimodal blend. These polymer blends, made as “controls”, are also shown in Table 6 and Figure 7.

Finally, in method C, the two metallocenes were mixed together in a single solution in an intimate combination and

**Figure 7.** MW distributions of polymers made with two metallocene-derived components.

then coimpregnated onto a single activator support. Bimodal polymers were then made from these dual-component catalysts and are designated “catalyst blends” in Figures 7 and 8.

The zero-shear melt viscosity is shown in the power-law plot in Figure 8. Notice that the two individual components made by method A showed very little elasticity. The low-MW component would not be expected to exhibit high viscosity, even if it were high in LCB, because of the Janzen–Colby dependence on MW. The high-MW component was also low in elasticity, signifying that it was low in LCB. One possible explanation is the extremely high MW yields a scarcity of vinyl end-groups, or macromer.

The bimodal polymer blends made by method B are also shown in Figure 8. As expected, they do not show an increase in viscosity relative to their MW. Blending linear or non-viscous polymers may broaden the MW distribution but it does not increase the melt viscosity relative to that MW.

As demonstrated in Figure 7, both high-MW and low-MW producing sites contributed to the MW distribution in method C. Active sites were intimately mixed, residing only Angstroms away from each other. Thus, coimpregnating the two metallocenes should greatly increase the population of vinyl end-groups available to the high-MW-producing metallocene sites. Vinyl concentrations, from NMR spectroscopy and GPC measurements, are listed in Table 6. Since hydrogen was not used to control molecular weight in these experiments, chain end-groups from the low-MW-producing component contained high levels of vinyl end-groups. Despite the low MW, however, the low-MW-producing metallocene was chosen so that almost all of these chains would be longer than the critical entanglement length of 140 carbons, necessary to be rheologically significant.^{21–23,26} The viscosity of these bimodal polymers is dominated by the high-MW component. Therefore, any resulting increase in LCB incorporation by the metallocene producing high MW should be easily detectable by a sharp increase in low shear melt viscosity, since it is always dominated by LCB in the high-MW region.²² However, Figure 8 shows that there is no increase in viscosity. The bimodal samples derived from mixing metallocenes were no more viscous than the mixed polymer controls. This indicates that the high-MW-producing metallocene did not incorporate chains generated by the low-MW-producing metallocene, even though they were formed in abundance. SEC–MALS experiments also indicated no major difference between the polymer blend samples made by method B and those made from mixed metallocenes in method C. [On close

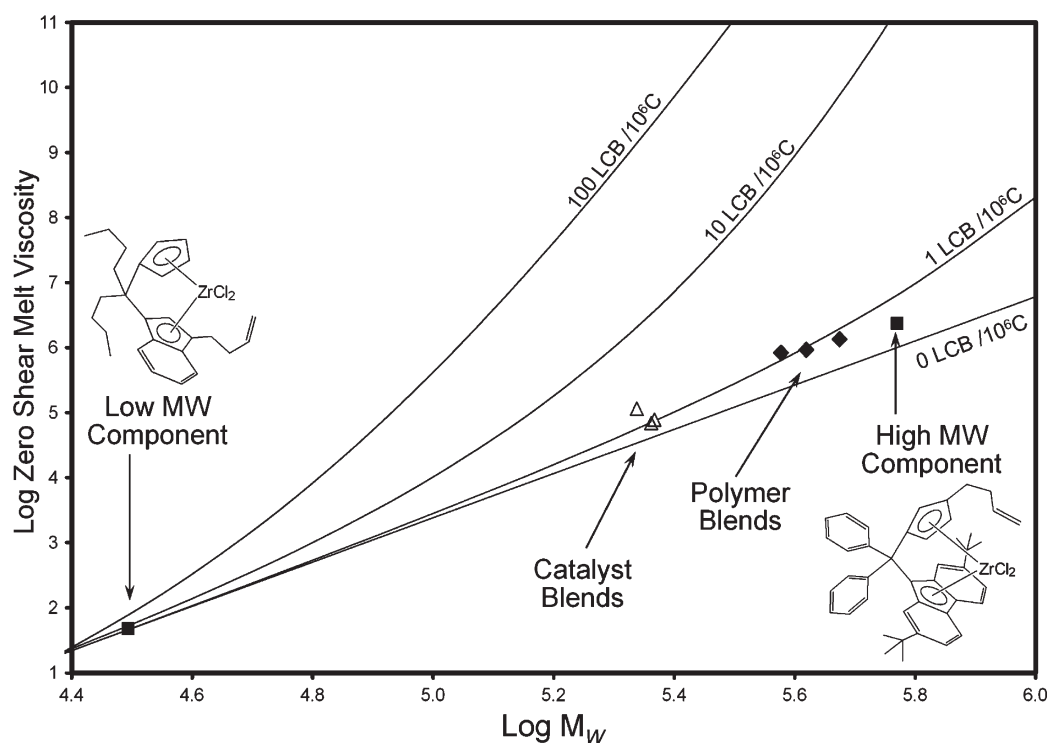
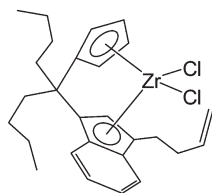


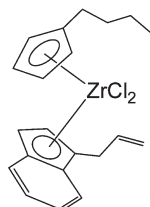
Figure 8. Janzen–Colby plot of polymers made from two metallocene-derived components.

Table 7. LCB from Catalysts Containing Two Metallocene-Derived Components^a

Low MW Catalyst



High MW Catalyst



% components			term-vinyl			JC-α LCB/ 10 ⁶ C
high MW	low MW	mol wt M _w /1000	per 1000C ^b	per chain ^b	mol/L ^c	
100	0	197	0.09	0.44	0.030	1.5
0	100	31	1.29	1.08	0.162	3.2
25	75	67	0.37	0.51	0.111	2.5
30	70	76	0.46	0.56	0.124	3.1

^a Simultaneous production of two polymers through polymerization by a catalyst containing two metallocene components. ^b Based on NMR spectroscopy. ^c Based on GPC M_N , 1 vinyl per chain, and 62% amorphous

inspection one can see that the mixed metallocenes did not produce the same MW distribution as the blended polymer components. The high-MW component is not as high in MW. This is due to the well documented tendency of these metallocenes to generate H_2 during polymerization. In fact H_2 generated by the low-MW component reacts with the high-MW component, thus moving the two peaks closer together. This does not affect the LCB arguments being made here.] Therefore, there is no indication in this experiment of cross-insertion between sites.

This experiment was repeated with other metallocenes as well. In Table 7, an unbridged metallocene was used for the high-MW component. It also incorporates 1-hexene, although with

only about 25% of the efficiency of the high-MW-producing metallocene in Table 6. Solutions containing varying amounts of the two metallocenes in Table 7 were then impregnated onto the same activator support noted above, and used to polymerize ethylene. The results are listed in the table. (The MW distribution and Janzen–Colby viscosity plots are available in the Supporting Information as Figures S3 and S4). When compared to the high-MW-producing component alone, one can see in Table 7 that mixing the two metallocenes increased the terminal-vinyl concentration in the polymer by about 4–5 fold, compared to the high-MW component alone. Nevertheless, despite the much higher macromer concentration for the “catalyst blend”, once again this did not result in a significant increase in LCB concentration over what would be obtained from the “polymer blend” of the individual components. This is yet another example where no evidence of macromer cross-insertion between sites was found.

Still other metallocenes were also tested in this way, changing both the low- and high-MW components. Both bridged and unbridged metallocenes were used, some known for producing LCB and others not. In some experiments another way was also used of comparing the results from single versus mixed metallocenes. When running the high-MW component alone, hydrogen was added to the reactor to reduce the MW, but without adding to the terminal-vinyl population. This permitted direct comparison with the mixed metallocenes at a similar M_w . The results from these other experiments have been summarized in Table 8, and the GPC curves and Janzen–Colby viscosity plots are shown in Supporting Information, Figures S5–S15. Once again there was no indication of a major change in LCB formation when the vinyl concentration was increased by mixing metallocenes. This indicates that major cross-incorporation between sites of vinyl end-groups did not take place.

The cross-incorporation experiment was also repeated using a Ziegler catalyst, and the results are summarized in

Table 8. Other Experiments Using Two Components

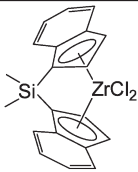
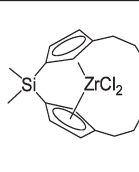
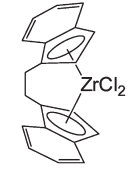
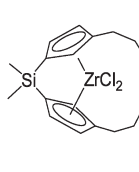
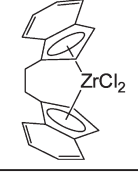
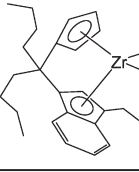
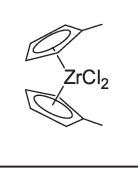
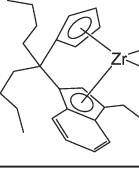
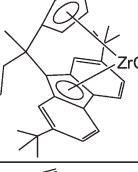
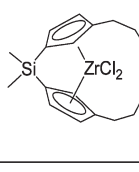
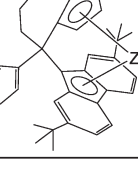
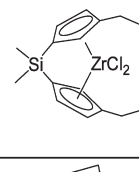


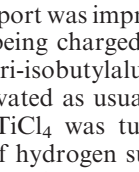
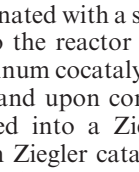
A (High MW)	B (Low MW)	Run	M _w /1000	LCB/10 ⁶ C	Figures
		B	40	4	Sup. Figure S5
		A + H ₂	130	65	
		A + B	131	19	
		A	169	10.5	Sup. Figures S6, S7
		B	43	3.1	
		A + H ₂	79	6.5	
		A + B	73	5.3	
		A	104	4.6	Sup. Figures S8, S9
		B	22	NA	
		A + B	66	1.1	
		A	204	2.0	Sup. Figures S10, S11
		B	22	NA	
		A + B	88	2.4	
		A + B	58	1.8	
		A	135	3.6	Sup. Figures S12, S13
		B	43	3.1	
		A + H ₂	108	3.4	
		A + B	110	4.1	
		A + H ₂	117	3.6	
		A	320	1.4	Sup. Figures S14, S15
		B	43	3.1	
		A + H ₂	116	1.8	
		A + B	123	1.4	
		A + H ₂	101	1.7	
		A	4000	0.1	Figures 9 & 10
		B	350	0.9	
		A + B	550	0.3	
		A + B	650	0.1	
		B + H ₂	245	1.4	
		A + B + H ₂	500	0.5	

Table 8. The activator support was impregnated with a small amount of TiCl₄ before being charged to the reactor with metallocene solution and tri-isobutylaluminum cocatalyst.⁹⁶ The metallocene was activated as usual, and upon contact with the cocatalyst the TiCl₄ was turned into a Ziegler catalyst. In the absence of hydrogen such Ziegler catalysts produce ultrahigh-MW polyethylene. Therefore, one can see the contribution of the TiCl₄ as a very high-MW tail to the otherwise narrow MW distribution. An example is shown in Figure 9.

Such Ziegler catalysts can incorporate 1-hexene comonomer, and in fact are used to manufacture most of the world's commercial LLDPE. Incorporation efficiency was 0.025, about 50–60% of that of the unbridged metallocenes in Table 3. However, such Ziegler catalysts do not produce LCB. This is usually attributed to the scarcity of vinyl end-groups. The naturally high MW is moderated by adding hydrogen to the reactor, which leaves saturated, rather than vinyl, end-groups. Used in combination with a metallocene

catalyst, however, the possibility exists that a Ziegler site could incorporate vinyl-terminated chains from a neighboring metallocene site.

The viscosity results are plotted in Figure 10, using the metallocene shown. This metallocene produces considerably lower MW polymer than the Ziegler catalyst, and with vinyl end-groups. Therefore, because of the difference in molecular weight, the Ziegler catalyst now experiences a vinyl end-group population about 10 times higher than it would running alone. According to the Janzen–Colby relationship, if the Ziegler catalyst incorporates even a low amount of macromer from the metallocene component, its ultrahigh-MW would produce a large increase in melt viscosity. It can be seen in Figure 10 that this did not happen. The combined catalysts actually came closer to the linear reference line. This is expected if the Ziegler component is more linear than the metallocene. The metallocene LCB contribution is “diluted” by the linear Ziegler polymer. Because of its high MW, the Ziegler contribution

tends to have a disproportionate influence on the combined viscosity. SEC–MALS also indicated low LCB in the metallocene peak, and linear PE from the Ziegler contribution. Therefore, once again, there is no evidence for cross-incorporation.

This experiment was repeated several times using both the Janzen–Colby and SEC–MALS methods to detect the presence of LCB. Again, however, we were unable to find any strong evidence of cross-insertion between sites.

Chromium Oxide Catalysts. Although it is not certain that these metallocene observations must also apply to the Phillips chromium based catalysts, there are many similarities. Phillips catalysts usually produce LCB and in some cases the levels can be quite high, based on rheological behavior. These catalysts produce broad MW distributions, with polydispersity up to 100, which should provide extreme opportunity for cross-insertion between sites if it is possible. Studying these catalysts for decades, we have often suspected that the LCB produced tends to be concentrated into the low-MW part of the MW distribution.

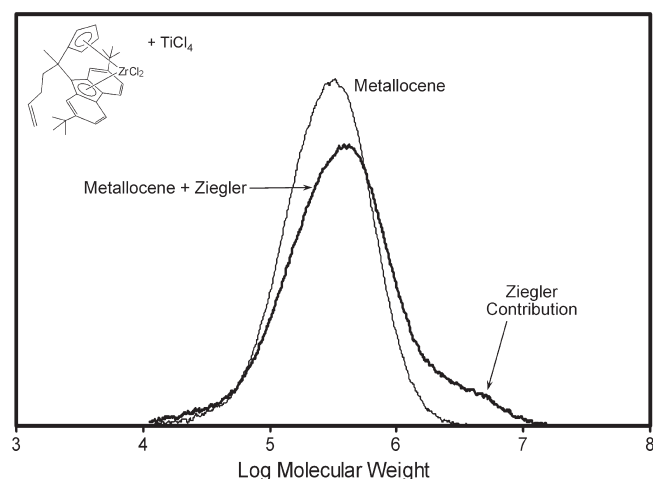


Figure 9. MW distribution of polymer made with catalyst containing both metallocene and Ziegler components.

Modifications of the catalyst that enhance the low-MW part of the distribution often also increase LCB. One example is Cr/aluminophosphate.^{10,11} The polymers produced by this catalyst have an exceptionally broad MW distribution, with polydispersity of 50–100. In an earlier report it was shown that, unlike Cr/silica, the alumina based catalysts tend to produce a flat SCB profile.^{97,98} That is, 1-hexene is incorporated equally into all parts of the MW distribution. Figure 11 shows the incorporation of 1-hexene in one experiment.

Alumina based catalysts tend to produce very low LCB levels, at least on average when referenced to their extremely high MW. Adding phosphate to the catalyst embellishes the low-MW region around 10^4 , and LCB levels simultaneously increase significantly. Overall elasticity in the polymer correlates well with the amount of phosphate in the catalyst.^{10,11} In an effort to probe the LCB content of the low-MW region from these catalysts, a polymer was solvent-fractionated into components, each having a polydispersity of from about 1.1 to 1.8. These fractions were then analyzed by the usual rheological method, and also by SEC–MALS. The results are shown in Figure 11. SEC–MALS gives somewhat higher LCB values than the Janzen–Colby technique, perhaps partly because SEC–MALS gives LCB as a direct function of MW, whereas rheology gives an average LCB level for each fraction. However, it is quite clear from either type of measurement that LCB does concentrate into the low-MW region of this polymer, even though the catalyst exhibits no such discrimination for 1-hexene incorporation.

This is yet another example where incorporation of LCB does not parallel that of SCB. The results also imply that cross-incorporation did not occur. Otherwise, the sites producing high MW, which incorporated 1-hexene well, should have incorporated macromers generated on the sites producing the low-MW chains, where most of the vinyl end-group population was concentrated. This experiment, and other observations,^{9–11} suggests that Phillips chromium oxide based catalysts also exhibit selectivity in the formation of LCB.

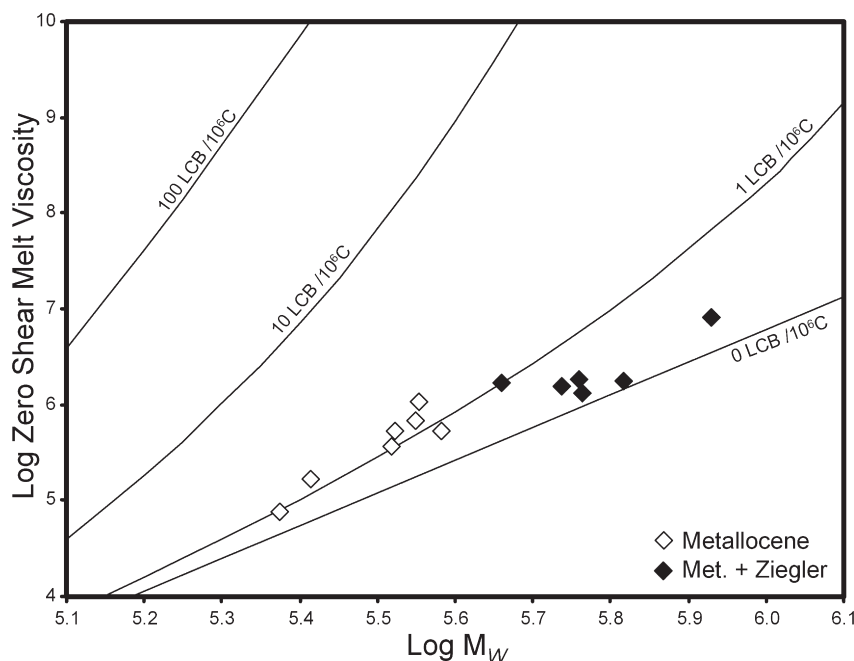


Figure 10. Janzen–Colby plot of polymers made with combined metallocene + Ziegler catalyst.

Metallocene Precipitation with Polymer. Although metallocene structure affects both SCB and LCB incorporation, it is clear that they follow independent paths. The most glaring evidence for this is the effect of tethered olefinic substituents, such as shown in Table 4, where the metallocene possessing a pendant olefin is compared with its saturated analogue. The pendant olefin had no effect on SCB but does shut down LCB. ^{16,49,51} This suggests that the tethered olefins displace or prevent insertion of coordinated macromer. A mechanism consistent with this observation was presented in Scheme 3. Once the macromer is dissociated, it may be difficult for the “solidified” chain end to find the site again and re-coordinate. Thus, unlike comonomer, desorption of macromer may be essentially irreversible. Adding comonomer to the reactor can also decrease LCB formation. ^{4,7,34,37,38} Both comonomer and tethered olefinic substituents significantly enhance the activity, which is consistent with their role as a coordinating “activator” ligand.

Others have presented an alternative function for this pendant olefin. They claim that the olefinic pendant serves as monomer in a so-called “self-immobilization” mechanism to afford a heterogeneous metallocene catalyst. ^{15,99–110} According to this view, which is illustrated in Scheme 4, the pendant olefin copolymerizes with ethylene into the polymer chain, thus changing into a larger polymeric substituent whereby the unsaturation of the pendant no longer exists. ^{99–102,110}

The published evidence for this has been presented in a series of remarkable photos, including those adorning the cover of one journal. ¹⁰¹ In these, the color of metallocene/MAO/toluene solutions disappears from solution once ethylene is introduced and polymer is precipitated out of solution. Indeed, only the precipitated polymer possesses color, not the solution, thus indicating that the metallocene catalyst has been “immobilized” or “heterogenized”.

Obviously, the mechanism proposed in Scheme 3 requires that the pendant olefin remain intact during polymerization and precipitation. Models of the third metallocene in

Table 4 (and cited as a commercial example of “self immobilization” ^{15,102}) suggest that *intramolecular* carbozirconation of the pendant butenyl group would not be favorable. Alternatively, given the large molar mass of MAO-bound metallocene centers, incorporation of the pendant olefin on one metallocene by a second catalytic center in solution also seems entropically unfavorable. [Contrary to the figures often depicted, ^{99–102,106,110} if only *intramolecular* self-copolymerization of the tether with ethylene occurs, then only one incorporation per chain is possible.] Moreover, given the very low concentration of metallocene present in the reaction mixture, compared to the monomer or comonomer, *intermolecular* incorporation of one metallocene by another is unlikely. Therefore, reinvestigation of the observed color changes in the self-immobilization procedure is warranted.

Accordingly, the third metallocene in Table 4, containing the butenyl pendant, was treated with MAO in a 1:2000 molar ratio (Zr:Al) in toluene solvent. The polymerization was conducted at 25 °C and 1.4 atm of ethylene. After several grams of PE had been generated, the polymer was then centrifuged to the bottom of the bottle, leaving a clear colorless liquid above. In contrast, the precipitated polymer was violet-red, indicating that the metallocene had come down with it. Attempts to precipitate and remove the metallocene/MAO catalyst by centrifugation prior to polymer formation were unsuccessful. These results are consistent with those reported earlier by Alt et al. ¹⁰¹

As a control, this procedure was then repeated, except that the second metallocene in Table 4 was used. That is, the metallocene bridge possessed a butyl, instead of a butenyl, substituent. Otherwise the two metallocenes were identical. It was added along with MAO in a 1:2000 molar ratio (Zr:Al) and toluene as before. Ethylene was added, and after several grams of PE had been generated, the polymer was centrifuged to the bottom of the bottle. Once again, a clear colorless liquid was left as the supernatant, while all the color went down with the precipitate. Therefore, the second metallocene in Table 4, which had a saturated tether, was also brought down with the polymer, and could be clearly seen as a red-violet solid. This is shown in Figure 12. The first metallocene in Table 4 was also tested in an identical fashion, with the same result. In these experiments, however, self-polymerization with ethylene is not a viable explanation for the phenomenon.

In contrast to the self-immobilizing mechanism depicted in Scheme 4, these observations appear to be consistent with the mechanism of LCB formation depicted in Schemes 2 and 3, i.e., that the macromer remains coordinated to the metallocene, and thus can be dragged down with insoluble polymer. When considering the *intramolecular* mechanism of Scheme 2, it is only necessary that the terminated macromer remain coordinated long enough for another chain to grow—typically a few tenths of a second. In these experiments, however, after essentially complete consumption of ethylene, the polymer may remain attached to the metallocene

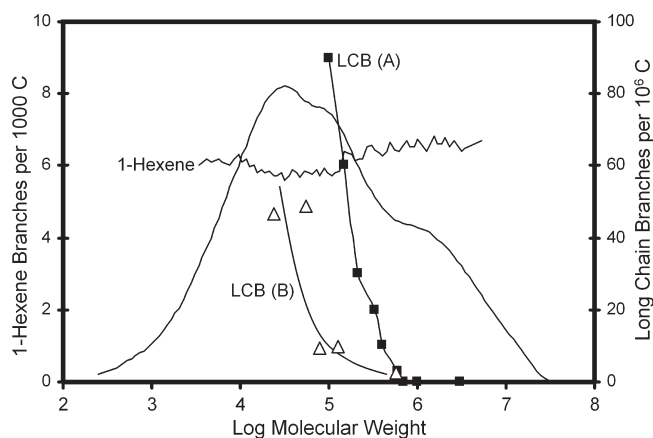
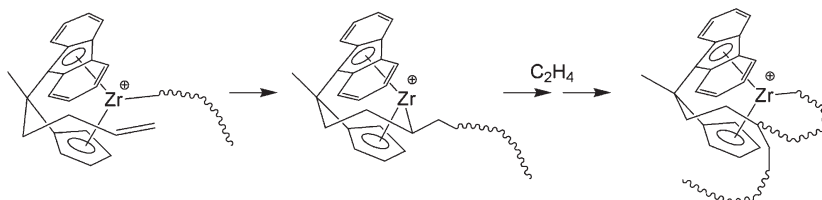


Figure 11. LCB and SCB placement by a modified Cr/alumina catalyst. LCB determined from fractionated components by (A) SEC–MALS and (B) rheology.

Scheme 4. Previously Assumed “Self-Immobilization” by Incorporation of Pendant Olefin (See Refs 15, 101, and 102)



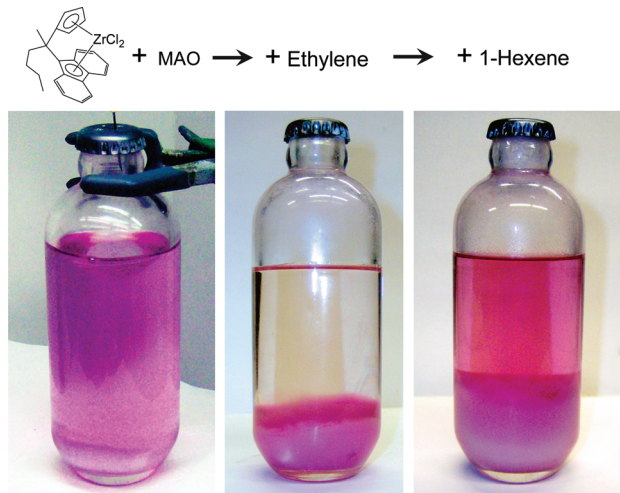


Figure 12. Metalocene precipitation with PE, then liberation by 1-hexene.

for hours or days. Indeed, the scarcity of monomer remaining in these experiments could have aided this attachment.

As noted earlier, macromer dissociation is probably irreversible, and LCB formation can be impeded by comonomer addition,^{4,7,34,37,38} perhaps suggesting that comonomer can displace, or replace, coordinated macromer at the active site. Indeed, adding a few mL of 1-hexene to the mixtures containing the centrifuged PE derived from metallocenes 1–3 in Table 4, immediately extracted the color back into solution. This also is shown in Figure 12. Moreover, once 1-hexene had been added to these mixtures, the color remained in solution despite further centrifugation. It indicates that the association between metallocene and precipitated polymer is reversible, and thus the butenyl group on the third metallocene in Table 4 did not copolymerize with ethylene. Rather the tendency of olefinic substituents to lower LCB^{16,49,51} probably occurs through coordination, such as depicted in Scheme 3. Both comonomer and tethered olefinic substituents significantly enhance the activity, which is consistent with their role as a coordinating “activator” ligand.

After introduction of ethylene and precipitation of PE, it is noteworthy that the presence of the butenyl substituent in the third metallocene in Table 4 was not sufficient to maintain color in the supernatant. Only by adding 1-hexene did color reappear in the supernatant. These results are consistent with Scheme 3, whereby the olefinic substituent does not directly displace macromer, but rather mitigates ethylene insertion and thus chain growth while it and macromer are coordinated. Indeed, 1-hexene may act in a similar role to inhibit chain growth, at least temporarily (before it undergoes insertion), requiring self-insertion or dissociation of macromer before chain growth via ethylene insertion can continue. However, at least in the case with a constrained butenyl group, unlike the substituent, 1-hexene is not in “infinite” concentration and can undergo insertion and is therefore less effective than the tether at mitigating LCB formation.

Conclusions

The widely accepted (*intermolecular*) mechanism of LCB formation does not adequately predict experimental observation. It is inconsistent with 1) the observed LCB response to common reactor variables, 2) the surprisingly high LCB incorporation efficiency, 3) the independent response of LCB and SCB to catalyst structure, and 4) the lack of cross-insertion between sites. Therefore, this mechanism needs to be revised or modified.

One possibility has been proposed—*intramolecular* incorporation, in which the terminated macromer remains coordinated to the active site even as a new chain grows on the same site. However, once the macromer dissociates from the site, it may be impossible for the solidified chain end to find the site again and re-coordinate. Thus, unlike comonomer coordination, dissociation of macromer may be irreversible. Evidence that the Zr site can coordinate two olefins during polymerization, and thus hold on to macromer, comes from kinetic responses and from simply watching the metallocene precipitate with the polymer. An *intramolecular* mechanism addresses all the problems cited above. It also explains the LCB response to specific metallocene structural changes, such as adding bulky or pendant olefinic substituents.

Intramolecular incorporation means that each site would incorporate mainly macromers produced by that same site. This significantly alters the expected polymer LCB architecture. Long chains would likely produce long branches, whereas *intermolecular* cross-insertion would produce mainly “combs”, i.e., long chains with short branches. In our experience the extreme elastic behavior produced by metallocenes, with some polymers even becoming essentially insoluble, is more consistent with *intramolecular* incorporation. Finally, it should be noted that these observations apply only to slurry, and possibly gas phase, polymerizations, where the macromer is frozen into the polymer matrix as it is formed. It is conceivable that *intermolecular* cross-insertion can occur under solution conditions, where the macromer is dissolved and mobile, free to react as any other monomer would. However, solution conditions generally provide lower LCB levels than slurry polymerization.^{2,9–11} This might be due to dilution of macromer concentration or to a weakening of the macromer coordination at the higher temperatures.

Acknowledgment. The authors wish to thank Dr. Joel Martin, Dr. Matt Thorn, and Dr. Kumi Jayaratne, formerly of the Chevron-Phillips Catalysis group. We are also indebted to Elizabeth Benham, Kathy Collins, Randy Muninger, and Tony Crain of the Chevron-Phillips Catalysis and Pilot Plant Groups, for making some of the polymers described herein, and to Dr. David Rohlffing and Dr. Ashish Sukhadia, of the Chevron-Phillips Polymer Analysis Group, for assistance interpreting rheological measurements. Dr. Youlu Yu performed SEC–MALS analysis, and Dr. Stephen J. Wharry obtained NMR measurements.

Supporting Information Available: Figures illustrating the GPC curves, Janzen–Colby plots, and VanGurp–Palmen plots of many other examples of catalyst or polymer mixtures. This material is available free of charge via the Internet at <http://pubs.acs.org>.

References and Notes

- Wang, W. J.; Yan, D.; Zhu, S.; Hamielec, A. E. *Macromolecules* **1998**, *31*, 8677–8683.
- Kolodka, E.; Wang, W. J.; Charpentier, P. A.; Zhu, S.; Hamielec, A. E. *Polymer* **2000**, *41*, 3985–3991.
- Gabriel, C.; Kokko, E.; Löfgren, B.; Seppälä, J.; Münstedt, H. *Polymer* **2002**, *43*, 6383–6390.
- Kokko, E. A.; Malmberg, A.; Lehmus, P.; Fgren, B. L.; Seppälä, J. V. *J. Polym. Sci. A: Polym. Chem.* **2000**, *38*, 376–388.
- Malmberg, A.; Liimatta, J.; Lehtinen, A.; Löfgren, B. *Macromolecules* **1999**, *32*, 6687–6696.
- Malmberg, A.; Gabriel, C.; Steffl, T.; Münstedt, H.; Löfgren, B. *Macromolecules* **2002**, *35*, 1038–1048.
- Villar, M. A.; Failla, M. D.; Quijada, R.; Mauler, R. S.; Valles, E. M.; Galland, G. B.; Quinzani, L. M. *Polymer* **2001**, 9269–9279.
- Ye, Z.; Alobaidi, F.; Zhu, S.; Subramanian, R. *Macromol. Chem. Phys.* **2005**, *206*, 2096–2105.
- McDaniel, M. P.; Rohlffing, D. C.; Benham, E. A. *Polym. React. Eng.* **2003**, *11*, 101–132.

- (10) McDaniel, M. P., *Polymerization on Phillips Type Catalysts, in Handbook of Heterogeneous Catalysis*, 2nd ed., Ertl, G., Knozinger, H., Schuth, F., Weitkamp, J., Eds.; Wiley-VCH Verlag: Weinheim, Germany, 2008, Chapter 15.1, pp 3733–3792.
- (11) McDaniel, M. P. *Adv. Catal.* **2010**, 53, 123–606.
- (12) McDaniel, M. P.; Collins, K. S. *J. Catal.* **2009**, 261, 34–49.
- (13) McDaniel, M. P.; Collins, K. S. *J. Polym. Sci., Part 1: Chem.* **2009**, 47, 845–865.
- (14) Jensen, M. D., Martin, J. L., McDaniel, M. P., Rohlffing, D. C., Yang, Q., Thorn, M. G., Benham, E. A., Cymbaluk, T. H., Sukhadia, A. M., Krishnaswamy, R. K., Kertok, M. E. U.S. Patent 7,119,153, issued October 10, 2006, to Chevron Phillips Chemical Company, L.P.
- (15) Fahey, D. R., Lauffer, D. E., Dockter, D. W., Das, P. K., Boudreaux, E., Whittle, W. M. Presented at the MetCon 99 Metallocene Conference, held in Houston, TX, June 9–10, 1999, by the Society of Plastics Engineers.
- (16) Jensen, M. D., Martin, J. L., McDaniel, M. P., Rohlffing, D. C., Yang, Q., Thorn, M. G., Sukhadia, A. M., Yu, Y., Lanier, J. T. U.S. Patent 7,148,298, issued December 12, 2006, to Chevron Phillips Chemical Company, L.P.
- (17) McDaniel, M. P., Jensen, J. D., Jayaratne, K., Collins, K. S., Benham, E. A., McDaniel, N. D., Das, P. K., Martin, J. L., Yang, Q., Thorn, M. G., Masino, A. P. *Metallocene Activation by Solid Acids*. In *Tailor-Made Polymers*; Severn, J. R., Chadwick, J. C., Eds.; Wiley-VCH Verlag GmbH & Co.: Weinheim, Germany, 2008, XVI, Chapter 7, pp 171–210.
- (18) McDaniel, M. P., Collins, K. S., Eaton, A. P., Benham, E. A., Jensen, M. D., Martin, J. L., Hawley, G. R. U.S. Patent 6,355,594, issued March 12, 2002, and U.S. Patent 6,613,852, issued September 2, 2003, both to Chevron Phillips Chemical Company, L.P.
- (19) McDaniel, M. P., Benham, E. A., Martin, S. J., Smith, J. L., Collins, K. S. U.S. Patent 6,300,271, issued October 9, 2001, to Chevron Phillips Chemical Company, L.P.
- (20) McDaniel, M. P., Benham, E. A., Martin, S. J., Smith, J. L., Collins, K. S., Hawley, G. R., Wittner, C. E., Jensen, M. D. U.S. Patent 6,831,141, issued December 14, 2004, to Chevron Phillips Chemical Company, L.P.
- (21) Bird, R. B., Armstrong, R. C., Hassager, O. *Dynamics of Polymeric Liquids, Vol. 1, Fluid Mechanics*; John Wiley & Sons: New York, 1987.
- (22) Janzen, J.; Colby, R. H. *J. Mol. Struct.* **1999**, 485–486, 569–584.
- (23) Fetters, J., Lohse, D. J., Colby, R. H. In *Physical Properties of Polymers Handbook*; Mark, J. E., Ed.; AIP Press: New York, 1996; pp 335–340.
- (24) Stadler, F. J.; Piel, C.; Kaschta, J.; Rulhoff, S.; Kaminsky, W.; Münstedt, H. *Rheol. Acta* **2006**, 45, 755–764.
- (25) Stadler, F. J.; Münstedt, H. *Macromol. Mater. Eng.* **2008**, 293, 907–913.
- (26) Arnett, R. L.; Thomas, C. P. *J. Phys. Chem.* **1980**, 84, 649–652.
- (27) Yau, W. W. *Polymer* **2007**, 48, 2362–2370.
- (28) Yu, Y.; Deslauriers, P. J.; Rohlffing, D. C. *Polymer* **2005**, 46, 5165–5182.
- (29) Kaye, W.; McDaniel, J. B. *Appl. Opt.* **1974**, 13, 1934–1937.
- (30) Fox, T. G.; Flory, P. J. *J. Am. Chem. Soc.* **1951**, 73, 1904–1908.
- (31) Ptitsyn, O. B.; Eizner, Yu. E. *Sov. Phys. Tech., Phys.* **1960**, 4, 1020–1036.
- (32) Wyatt, P. J. *Anal. Chim. Acta* **1993**, 272, 1–40.
- (33) American Polymer Standard, www.ampolymer.com. Note: At the run temperature, 145 °C, it was found that $dn/dc = 0.095 \text{ mL/g}$ by assuming refractive index changes linearly as a function of temperature and the polymer standard is 100% soluble.
- (34) Malmberg, A.; Kokko, E.; Lehmus, P.; Löfgren, B.; Seppälä, J. V. *Macromolecules* **1998**, 31, 8448–8454.
- (35) Stadler, F. J.; Piel, C.; Kaminsky, W.; Münstedt, H. *Macromol. Symp.* **2006**, 236, 209–218.
- (36) Piel, C.; Stadler, F. J.; Kaschta, J.; Rulhoff, S.; Münstedt, H.; Kaminsky, W. *Macromol. Chem. Phys.* **2006**, 207, 26–38.
- (37) Stadler, F.; Piel, C.; Klimke, K.; Kaschta, J.; Parkinson, M.; Wilhelm, M.; Kaminsky, W.; Münstedt, H. *Macromolecules* **2006**, 39, 1474–1482.
- (38) Walter, P.; Trinkle, S.; Suhm, J.; Mäder, D.; Friedrich, D.; Mühlaupt, R. *Macromol. Chem. Phys.* **2000**, 201, 604–612.
- (39) Soares, J. B. O. *Macromol. Theory Simul.* **2002**, 11, 184–198.
- (40) Mohring, P. C.; Coville, N. J. *Coord. Chem. Rev.* **2006**, 250, 18–35.
- (41) Yang, Q., *Synthesis and Behavior of C3 and C4 Bridged Indenyl Metallocene Catalysts*, Society of Plastics Engineers RETECH Meeting, Feb. 2004, held in Houston, TX.
- (42) Yang, Q., Jensen, M. D., Steinhart, P., Johnson, A., *Book of Abstracts*, 213th ACS National Meeting, San Francisco, CA, April 13–17, 1997; American Chemical Society: Washington, DC, 1997.
- (43) Erker, G.; Aulbach, M.; Knickmeier, M.; Wingbermühle, D.; Krüger, C.; Nolte, M.; Werner, S. *J. Am. Chem. Soc.* **1993**, 115, 4590–4601.
- (44) Piemontesi, F.; Camurati, I.; Resconi, L.; Balboni, D. *Organometallics* **1995**, 14, 1256–1266.
- (45) Linnolahti, M.; Pakkanen, T. A.; Leino, R.; Luttikhedde, H. J. G.; Wilen, C. E.; Näsman, J. H. *Eur. J. Inorg. Chem.* **2001**, 2033–2040.
- (46) Welborn, H. C.; Sagar, V. R.; Poirot, E. E.; Canich, J. A. M.; Burkhardt, T. J. World Patent 96/00246, filed June 24, 1994, by Exxon Chemical Co.
- (47) Floyd, J. C.; Jejelowo, M.; Crowther, D. J.; Vaughn, G. A.; Lue, C. T. World Patent 98/02470, Filed July 16, 1996, by Exxon Chemical Co.
- (48) Jejelowo, M. O.; Bamberger, R. L. U.S. Patent 5,470,811, issued Nov. 28, 1995, to Exxon Chemical Co.
- (49) Jensen, M. D., Martin, J. L., McDaniel, M. P., Rolfing, D. C., Yang, Q., Thorn, M. G., Sukhadia, A. M., Yu, Y., Lanier, J. T. U.S. Patent 7,148,298, issued December 12, 2006, to Chevron-Phillips Chemical Co.
- (50) Zimm, B. H.; Stockmayer, W. H. *J. Chem. Phys.* **1949**, 17, 1301–1314.
- (51) Yang, Q., Jensen, M. D., Martin, J. L., Thorn, M. G., McDaniel, M. P., Yu, Y., Rohlffing, D. C. U.S. Patent 7,517,939, issued April 14, 2009, to Chevron Phillips Company.
- (52) Köppl, A.; Alt, H. G. *J. Mol. Catal. A: Chem.* **2001**, 165, 23–32.
- (53) Yang, Q., McDaniel, M. P., Martin, J. L. U.S. Patent Application No. 210843, filed Sept. 28, 2007, assigned to Chevron-Phillips Chemical Co.
- (54) Kissin, Y. V.; Beach, D. L., *J. Polym. Sci., Part A* **1984**, 22, 233–240.
- (55) Nele, M.; Soares, J. B. P. *Polym. Prepr. (Am. Chem. Soc., Div. Polym. Chem.)* **2002**, 43 (1), 252–253.
- (56) Green, J. C. *Chem. Soc. Rev.* **1998**, 27, 263–271.
- (57) Karl, J.; Dahlmann, M.; Erker, G.; Bergander, K. J., *Am. Chem. Soc.* **1998**, 120, 5643–5652.
- (58) Lauher, J. W.; Hoffman, R. J. *Am. Chem. Soc.* **1976**, 98, 1729–1742.
- (59) Lin, M.; Spivak, G. J.; Baird, M. C. *Organometallics* **2002**, 21, 2350–2352.
- (60) Ystenes, M. J. *Catal.* **1991**, 129, 383–401.
- (61) Ystenes, M. *Makromol. Chem., Macromol. Symp.* **1993**, 66, 71–74.
- (62) Sukhadia, A. M.; Rohlffing, D. C.; Johnson, M. B.; Wilkes, G. L. *J. Appl. Polym. Sci.* **2002**, 85, 2396–2411.
- (63) Sukhadia, A. M., *Annu. Tech. Conf.-Soc. Plast. Eng.*, **2002**, 2, 1481–1486.
- (64) Das, P. K., Lauffer, D. E., Fahey, D. R., Palackal, S. J., Welch, M. B. *Book of Abstracts*, 215th ACS National Meeting, Dallas, March 29–April 2, 1998; American Chemical Society: Washington, DC, 1999.
- (65) Caporaso, L.; Galdi, N.; Oliva, L.; Izzo, L. *Organometallics* **2008**, 27, 1367–1371.
- (66) Izzo, L.; Caporaso, L.; Senatore, G.; Oliva, L. *Macromolecules* **1999**, 32, 6913–6916.
- (67) Izzo, L.; De Riccardis, F.; Alfano, C.; Caporaso, L.; Oliva, L. *Macromolecules* **2000**, 34, 2–4.
- (68) Melillo, G.; Izzo, L.; Zinna, M.; Tedesco, C.; Oliva, L. *Macromolecules* **2002**, 35, 9256–9261.
- (69) Koivumäki, J.; Seppälä, J. V. *Macromolecules* **1994**, 27, 2008–2012.
- (70) Koivumäki, J.; Fink, G.; Seppälä, J. V. *Macromolecules* **1994**, 27, 6254–6258.
- (71) Kissin, Y. V.; Mink, R. I.; Nowlin, T. E. *J. Polym. Sci.: Part A, Polym. Chem.* **1999**, 37, 4255–4272.
- (72) Calabro, D. C.; Lo, F. Y. In *Transition Metal Catalyzed Polymerizations: Ziegler Natta and Metathesis Reactions*; Quirk, R. P., Ed.; Cambridge University Press: New York, 1988; pp 729–739.
- (73) Kissin, Y., Mink, R., Nowlin, T., Brandolini, A., *Top. Catal.* **1999**, 7 (1–4), 69–88.
- (74) Burfield, D. R.; McKenzie, I. D.; Tait, P. J. T. *Polymer* **1976**, 17, 130–136.
- (75) Kissin, Y. V. *J. Mol. Catal.* **1989**, 56, 220–236.
- (76) Karol, F. J.; Kao, S. C.; Cann, K. J. *J. Polym. Sci., Part A: Polym. Chem.* **1993**, 31, 2541–2553.
- (77) Tait, P. J. T. In *Transition Metal Catalyzed Polymerizations: Ziegler Natta and Metathesis Reactions*; Quirk, R. P., Ed.; Cambridge University Press: New York, 1988; pp 834–860.
- (78) Busico, V.; Cipullo, R.; Cuttillo, F.; Vacatello, M. *Macromolecules* **2002**, 35, 349–354.

- (79) Thorshaug, K.; Støvneng, J. A.; Rytter, E.; Ystenes, M. *Macromolecules* **1998**, *31*, 7149–7165.
- (80) Chien, J. C. W.; Yu, Z.; Marques, M. M.; Flores, J.; Rausch, M. D. *J. Polym. Sci.: Part A, Polym. Chem.* **1998**, *36*, 319–328.
- (81) Pino, P.; Rotzinger, B.; von Achenbach, E. *Makromol. Chem. Suppl.* **1985**, *13*, 105–122.
- (82) Siedle, A. R.; Lamanna, W. M.; Olofson, J. M.; Nerad, B. A.; Newmark, R. A. *Selectivity in Catalysis*; ACS Symposium Series 517; American Chemical Society: Washington, DC, 1993; pp 156–167.
- (83) Read, D. J.; Soares, J. B. P. *Macromolecules* **2003**, *36*, 10037–10051.
- (84) Beigzadeh, D.; Soares, J. B. P.; Duever, T. A. *Macromol. Symp.* **2001**, *173*, 179–194.
- (85) Beigzadeh, D.; Soares, J. B. P.; Duever, T. A. *Macromol. Rapid Commun.* **1999**, *20*, 541–545.
- (86) Beigzadeh, D.; Soares, J. B. P.; Hamielec, A. E. *J. Appl. Polym. Sci.* **1999**, *71*, 1753–1770.
- (87) Beigzadeh, D.; Soares, J. B. P.; Hamielec, A. E. *Polym. React. Eng.* **1997**, *5*, 143–180.
- (88) Simon, L. C.; Soares, J. B. P. *Macromol. Theory Simul.* **2002**, *11*, 222–232.
- (89) Costeux, S. *Macromolecules* **2003**, *36*, 4168–4187.
- (90) Beigzadeh, D. *Macromol. Theory Simul.* **2003**, *12*, 174–183.
- (91) Iedema, P. D.; Hoefsloot, H. C. J. *Macromolecules* **2003**, *36*, 6632–6644.
- (92) Costeux, S. *Macromolecules* **2003**, *36*, 4168–4187.
- (93) Brant, P.; Canich, J. A. M.; Dias, A. J.; Bamberger, R. L.; Licciardi, G. F.; Henrichs, P. M. World Patent No. WO94/07930, published April 14, 1994.
- (94) Sperber, O.; Kaminsky, W. *Macromolecules* **2003**, *36*, 9014–9019.
- (95) Markel, E. J.; Weng, W.; Peacock, A. J.; Dekmezian, A. H. *Macromolecules* **2000**, *33*, 8541–8548.
- (96) McDaniel, M. P.; Collins, K. S.; Hawley, G. R.; Jensen, M. D.; Wittner, C. E.; Benham, E. A.; Eaton, A. P.; Martin, J. L.; Rohlfing, D. C.; Yu, Y., U.S. Patent 6,833,338, issued Dec. 21, 2004, and U.S. Patent 7,417,097, issued Aug. 26, 2008, both to Phillips Petroleum Company.
- (97) DesLauriers, P. J.; McDaniel, M. P.; Rohlfing, D. C.; Krishnaswamy, R. K.; Secora, S. J.; Benham, E. A.; Maeger, P. L.; Wolfe, A. R.; Sukhadia, A. M.; Beaulieu, W. B., *Polym. Eng. Sci.* **2005**, *45*, 1203–1213.
- (98) DesLauriers, P. J.; Tso, C.; Yu, Y.; Rohlfing, D. L.; McDaniel, M. P., *Appl. Catal.*, in press.
- (99) Alt, H., *Macromol. Symp.* **2001**, *173*, 65–75.
- (100) Alt, H. G. Supporting Metallocenes through Self Immobilization. In *Tailor-Made Polymers*; Severn, J. R., Chadwick, J. C., Eds.; Wiley-VCH Verlag GmbH & Co.: Weinheim, Germany, 2008; Vol. XVI, Chapter 12, pp 305–326.
- (101) Alt, H. G. *J. Chem. Soc., Dalton Trans.* **1999**, 1703–1709.
- (102) Alt, H. G. *J. Chem. Soc., Dalton Trans.* **2005**, 3271–3276.
- (103) Jung, M.; Alt, H. G.; Welch, M. B. U.S. Patent 5,886,202, issued March 23, 1999, to Phillips Petroleum Co.
- (104) WelchPeifer, B.; Palackal, S. J.; Glass, G. L.; Pettijohn, T. M.; Hawley, G. R.; Fahey, D. R. U.S. Patent 5,498,581, issued March 12, 1996, to Phillips Petroleum Co.
- (105) Alt, H. G.; Jung, M. *J. Organomet. Chem.* **1999**, *580*, 1–6.
- (106) Denner, C. E.; Alt, H. G. *J. Appl. Polym. Sci.* **2003**, *89*, 3379–3382.
- (107) Köppl, A.; Alt, H. G. *J. Mol. Catal.: A: Chem.* **2001**, *165*, 23–32.
- (108) Tang, G.; Jin, G. X.; Weng, L. *J. Organomet. Chem.* **2004**, *689*, 678–684.
- (109) Polo, E.; Forlini, F.; Bertolasi, V.; Boccia, A. C.; Sacchi, M. C. *Adv. Synth. Catal.* **2008**, *350*, 1544–1556.
- (110) Tang, G.; Jin, G. X.; Weng, L. *J. Organomet. Chem.* **2004**, *689*, 678–684.